arXiv:hep-th/0502113v2 6 Apr 2010

Multi-Flux Warped Throats and Cascading Gauge Theories

Sebastian Franco[†]**, Amihay Hanany**[†] **and Angel M. Uranga**[#] [∗]

[†]*Center for Theoretical Physics, Massachusetts Institute of Technology,*
Cambridge, MA 02139, USA.
`sfranco, hanany@mit.edu`
[#]*Instituto de Física Teórica, Facultad de Ciencias, C- XVI*
Universidad Autónoma de Madrid, 28049 Madrid, Spain
and TH Division, CERN, CH-1211 Geneve 23, Switzerland
`angel.uranga@uam.es, angel.uranga@cern.ch`

ABSTRACT: We describe duality cascades and their infrared behavior for systems of D3-branes at singularities given by complex cones over del Pezzo surfaces (and related examples), in the presence of fractional branes. From the gauge field theory viewpoint, we show that D3-branes probing the infrared theory have a quantum deformed moduli space, given by a complex deformation of the initial geometry to a simpler one. This implies that for the dual supergravity viewpoint, the gauge theory strong infrared dynamics smoothes out the naked singularities of the recently constructed warped throat solutions with 3-form fluxes, describing the cascading RG flow of the gauge theory. This behavior thus generalizes the Klebanov-Strassler deformation of the conifold. We describe several explicit examples, including models with several scales of strong gauge dynamics. In the regime of widely separated scales, the dual supergravity solutions should correspond to throats with several radial regions with different exponential warp factors. These rich throat geometries are expected to have interesting applications in compactification and model building. Along our studies, we also construct explicit duality cascades for gauge theories with irrational R-charges, obtained from D-branes probing complex cones over dP_1 and dP_2.

KEYWORDS: Quiver Gauge Theories, Duality Cascades.

Contents

1. Introduction

Much insight into the gauge/gravity correspondence has been obtained from the study of D3-branes at singularities. In the simplest situations where only regular D3-branes are present, the resulting gauge theories are conformal, and are dual to superstring backgrounds of the form $\text{AdS}_5 \times X_5$, where X_5 is the base of the real cone describing the singular manifold [1]. This has led to important extensions of the AdS/CFT correspondence to situations with reduced supersymmetry.

Conformal invariance can be broken by adding fractional D3-branes (e.g. D5-branes wrapped over collapsed 2-cycles at the tip of the singularity). The resulting renormalization group (RG) flow sometimes takes the form of a *duality cascade.* In a duality cascade, Seiberg duality is used to change to a dual description every time any of the gauge groups goes to infinite coupling. The idea of a cascading RG flow was first introduced in [2], for the gauge theory on D-branes over a conifold singularity.

The ultraviolet (UV) behavior of cascading theories is markedly different from that of ordinary field theories. Instead of having a UV fixed point, they have an infinite tower of dual theories with a steadily increasing number of colors and matter fields towards the UV. This increase can sometimes be linear as in [2], or can be much faster, with a power law or even exponential behavior. In the latter cases, the dualization scales generally present a UV accumulation point, leading to a duality wall [3, 4].

A supergravity solution describing the UV region of the conifold cascade was found by Klebanov and Tseytlin (KT) in [5]. This solution is well behaved at large energies but has a naked singularity in the infrared (IR). A full solution, which asymptotes the one of KT at large energies but is well behaved in the IR was later presented by Klebanov and Strassler (KS) in [2]. Instead of being based on the singular conifold, it is constructed using the *deformed conifold.* The 3-cycle inside the deformed conifold remains of finite size in the IR, avoiding the singular behavior. On the gauge theory side, the IR singularity is eliminated by strong coupling effects, whose scale is related to the dual 3-cycle size.

In [6], UV solutions, similar to that of KT, were constructed for complex cones over del Pezzo surfaces dP_n, for $3 \leq n \leq 8$. These supergravity solutions also suffer from the same problems in the IR. Contrary to what happens for the conifold, explicit metrics describing

either the non-spherical horizons or their deformations are not known. Therefore it remains an open question to develop methods to understand the infrared behavior of these theories in their dual versions. The purpose of this paper is to use the strong coupling dynamics of the dual gauge theories to extract as much information as possible regarding these deformations. In particular we will show a precise agreement between the field theory analysis of D3-branes probing the infrared of the cascades and the complex deformations of the initial geometries. This strongly supports the existence of completely smooth supergravity descriptions of the complete RG flow for (some of) these non-conformal gauge theories. In addition, our techniques are valid for other geometries, suggesting the existence of cascades and infrared deformations for other quiver gauge theories.

Although our examples are analogous to the conifold in some respects, the gauge theories and corresponding geometries are notably richer in others. For instance, we will encounter that these gauge theories generically give rise to several dynamical scales. In the regime of widely separated scales, the flow among these scales is to a great approximation logarithmic. The supergravity duals thus correspond to logarithmic throats with different warp factors, patched together at some transition scales. Clearly these topologically richer throats deserve further study.

Before proceeding, it is important to point out that our analysis shows that a smoothing of the singularity by a complex deformation may not be possible for some geometries, or even for all possible assignments of fractional branes in a geometry. Our methods give a clear prescription for when this is the case. A class of examples of this kind is provided by the countable infinite family of 5d horizons with $S^2 \times S^3$ topology, for which explicit metrics have been constructed in [7, 8, 9, 10, 11]. These geometries are labeled by two positive integers $p > q$ and are denoted $Y^{p,q}$. In [12], the quiver theories living on the world-volume of D3-branes probing metric cones over $Y^{p,q}$ geometries were derived. Impressive checks of the AdS/CFT correspondence for these models, such as matching the field theory R-charges and central charge $a = c$ with the corresponding geometric computations were carried out in full generality [12]. Recently, warped throat supergravity solutions dual to cascades in the $Y^{p,q}$ quivers were constructed in [13]. These solutions exhibit a naked singularity, and we show that for the particular subclass of $Y^{p,0}$ a complex deformation removes the IR singularity. However, in the general case these geometries do not admit complex deformations to smooth out their infrared behavior. It would be interesting to understand such examples, and we leave this question for future research.

The paper is organized as follows. In Section 2 we provide some background material. In section 2.1 we review the KS conifold. In section 2.2 we describe the supergravity throats

3

constructed in [6], and generalizations. In sections 2.3 and 2.4 we present a framework to determine possible geometric deformations for general local Calabi-Yau geometries using (p, q) web diagrams, and discuss a topological property of the corresponding RG flow solutions. In section 2.5 we introduce our approach to show that the strong gauge theory dynamics induces the complex deformation of the initial geometries to simpler ones. These arise as quantum deformations of the moduli space of the gauge theory describing D3-branes probing the infrared dynamics.

In Section 3 we describe some simple examples of RG cascading flows and infrared deformations, in several cases with a single strong dynamics scale. The examples include the cone over F_0, the cone over dP_2, and the suspended pinch point (SPP) singularity. In subsequent sections we present examples with several strong dynamics scales. In Section 4 we study the case of the cone over dP_3, which admits a two-scale deformation following the pattern $dP_3 \to$ conifold $\to$ smooth ($\mathbb{C}^3$). In Section 5 we present further two-scale examples, namely $dP_4 \to$ SPP $\to$ smooth, and $PdP_3 \to \mathbb{C}^2/\mathbb{Z}_2 \to$ enhançon.

Section 6 contains our concluding remarks. Appendix A presents an alternative approach for the field theory analysis of the mesonic branch, while Appendix B provides a detailed description of the deformations in toric geometry. Finally Appendix C describes the field theory description of the smoothing for real cones over the $Y^{p,0}$ manifolds.

2. Cascading throats

In this section we lay out our approach to cascading RG flows. We first discuss the supergravity duals that describe logarithmic flows, beginning with a review of the well known conifold example and then moving on to generalizations to other geometries. We then explain how to identify extremal transitions using (p, q) web diagrams. Finally, we discuss how these geometric deformations are generated by the strong coupling dynamics of the gauge theory.

2.1 Review of the conifold

To frame the forthcoming discussion, it is convenient to review the case of the conifold. The $\mathcal{N} = 1$ supersymmetric gauge theory on N D3-branes at a conifold singularity [1], in the presence of M fractional branes (i.e. D5-branes wrapped over the 2-cycle in the base of the conifold), is given by a gauge group $SU(N) \times SU(N + M)$, with two chiral multiplets A_1, A_2 in the representation $(\square, \overline{\square})$ and two multiplets B_1, B_2 in the representation $(\overline{\square}, \square)$. The superpotential is $W = A_1 B_1 A_2 B_2 - A_1 B_2 A_2 B_1$. In order to keep the notation short, we leave

the superpotential couplings and the trace over color indices implicit. We will adopt this convention when presenting all the forthcoming superpotentials.

As discussed in [2], for $M \ll N$ the theory undergoes a duality cascade as it flows to the infrared, at each step of which the highest rank gauge group becomes strongly coupled and is replaced by its Seiberg dual. Since the gauge theory of the conifold is self-dual (up to a modification of the gauge group ranks),[2] the cascade is fully specified by the sequence of gauge groups

$$SU(N) \times SU(N+M) \to SU(N) \times SU(N-M) \to SU(N-2M) \times SU(N-M) \to \dots$$

which shows that the number of effective D3-branes decreases along the flow, while the number of fractional branes, given by the difference in ranks between the two gauge groups, remains constant and equal to M. The cascade proceeds until this number is comparable with M. For N a multiple of M, the infrared theory has chiral symmetry breaking and confinement, and shares some features with $\mathcal{N} = 1 \, SU(M)$ SYM. Besides the heuristic field theory arguments, this picture is strongly supported by the dual supergravity solutions, which we now turn to describe.

In the absence of fractional branes the gauge theory on D3-branes at a conifold singularity is superconformal, and its supergravity dual is given by Type IIB theory on $\text{AdS}_5 \times T^{1,1}$. The 5-manifold $T^{1,1}$ is topologically $S^2 \times S^3$, and may be regarded as an S^1 fibration over $S^2 \times S^2$. Denoting σ_i the 2-forms dual to the two S^2's, we define for future convenience the Kähler class $\omega = \sigma_1 + \sigma_2$ and the orthogonal combination $\phi = \sigma_1 - \sigma_2$.

In the presence of M fractional branes, conformal invariance of the gauge theory is broken, and the supergravity dual is no longer $\text{AdS}_5 \times T^{1,1}$. In the UV, the supergravity dual is a particular case of the throats to be described in section 2.2. Sketchily, it is a warped version of $\text{AdS}_5 \times T^{1,1}$, with warping sourced by non-trivial RR and NSNS 3-form fluxes supported on ϕ,

$$G_3 = F_3 - \frac{i}{g_s}H_3 = M(\eta + i\frac{dr}{r}) \wedge \phi \qquad (2.1)$$

where η is a 1-form along the S^1 fiber in $T^{1,1}$, and r is the radial coordinate. In intuitive terms, the RR flux (related to F_3) is sourced by the fractional branes in the dual description, while the NSNS flux (related to H_3) leads to a logarithmic running of the relative inverse squared gauge coupling of the field theory. The fluxes also lead to a radially varying integral of the 5-form over $T^{1,1}$, which reproduces the decrease in the number of D3-branes in the

---

[2]Strictly speaking the term self-dual is exact at the conformal point for $M = 0$. This notion of self-duality is then borrowed to the case $M \neq 0$, where the superpotential stays the same while the ranks are changed.

duality cascade of the field theory. The solution does not contain, even asymptotically, an AdS_5. This is accordance with the fact that the gauge theory does not have a conformal fixed point in the presence of fractional branes.

The above solution, first studied in [5], if extended to the IR, leads to a naked singularity. Intuitively, this is because the above supergravity description misses the strong coupling dynamics taking place near the end of the cascade. The full solution in [2] is smooth, due to a non-trivial modification of the above ansatz in the infrared. In the IR, the geometry is a deformed conifold, and has a finite size S^3, which supports the RR 3-form flux. The size of this 3-cycle is related to the scale of strong dynamics of the dual gauge theory. The complete solution is a warped deformed conifold, with imaginary self-dual 3-form fluxes which are moreover $(2, 1)$-forms and thus preserve supersymmetry [15, 16]. In the UV, the full solution asymptotes the warped version of $\text{AdS}_5 \times T^{1,1}$ described above, while in the IR it contains a non-trivial 3-cycle supporting the flux.

Overall, the gauge/gravity correspondence is a relation between the field theory, described by fractional D3-branes on (i.e. D5-branes on the 2-cycle of) a resolved conifold, and the supergravity solution, described by 3-form fluxes on a deformed conifold. Namely a brane-flux transition taking place between two geometries related by an extremal transition where a 2-cycle disappears and is replaced by a 3-cycle [17, 18, 19, 20]. In our case the geometries under consideration are toric, and can be visualized using web or toric diagrams [21, 22]. The geometric interpretation of webs is discussed in detail in [23]. In these pictures, finite segments and faces of the initial web correspond to 2- and 4-cycles in the resolution phase, while 3-cycles correspond to segments joining the different sub-webs in the deformation phase. The geometrical transition is nicely depicted using web diagrams for the conifold geometry, as shown in Figure 1. The detailed geometric description of the deformation is described in Appendix B.
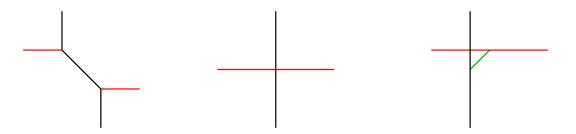

Figure 1: Conifold extremal transition. The finite segment in the first figure represents an S^2, with an area proportional to the length of the segment, while the green segment in the last figure corresponds to an S^3 with a volume proportional to the distance between the two infinite lines.

For future convenience, it is useful to review the matching between the deformation of the geometry and the infrared dynamics of the field theory. In particular, and following [2], we may recover the deformed conifold geometry as the moduli space of D3-branes probing the infrared end of the cascade.

A simple derivation follows by considering the infrared theory in the presence of M additional D3-branes. This is described by a conifold gauge theory with gauge group $SU(2M) \times SU(M)$, with the chiral multiplets A_r, B_r, $r = 1, 2$ and superpotential $W = A_1 B_1 A_2 B_2 - A_1 B_2 A_2 B_1$. The non-perturbative dynamics may be determined by assuming, to begin with, that the $SU(M)$ gauge factor is weakly coupled and acts as a spectator, corresponding to a global flavor symmetry. Then the gauge factor $SU(2M)$ has $N_f = N_c$ and develops a quantum deformation of its moduli space. Introducing the four mesons $M_{rs} = A_r B_s$, which transform in the adjoint of $SU(M)$, and the baryons $\mathcal{C}$, $\tilde{\mathcal{C}}$, the quantum modified moduli space is described by

$$\det(M_{11}) \det(M_{22}) - \det(M_{12}) \det(M_{21}) - \mathcal{C}\tilde{\mathcal{C}} = \Lambda^{4M}, \tag{2.2}$$

where Λ is the dynamical scale of the $SU(2M)$ gauge theory. The constraint may be implemented in the superpotential by introducing a Lagrange multiplier chiral field X, so it reads

$$W = M_{11} M_{22} - M_{12} M_{21} - X(\det \mathcal{M} - \mathcal{C}\tilde{\mathcal{C}} - \Lambda^{4M}), \tag{2.3}$$

with $\mathcal{M}$ a $2M \times 2M$ matrix whose blocks are the $M \times M$ matrices, $M_{11}, M_{12}, M_{21}, M_{22}$. The quantum constraint forces some of the mesons or baryons to acquire vevs. As discussed in [2], the dynamics of the probes is obtained along the mesonic branch[3], which corresponds to

$$X = \Lambda^{4-4M} \quad ; \quad \mathcal{C} = \tilde{\mathcal{C}} = 0 \quad ; \quad \det \mathcal{M} = \Lambda^{4M} \tag{2.4}$$

The vacuum is parametrized by the vevs of the mesons M_{ij}, subject to the quantum constraint. This can be seen to correspond to M D3-brane probes moving in a deformed conifold. To make this more manifest and to simplify the discussion, it is convenient to restrict to the Abelian case. This is sensible, because all the information about the non-Abelian gauge dynamics has been already included, and because we are not turning on

---

[3] As mentioned already in [2], the baryonic branch describes instead the continuation of the cascade down to the endpoint $SU(M)$ theory. That the infrared theory at the end of the cascade is in the baryonic branch is supported by the identification in the supergravity solution of the Goldstone mode associated to the spontaneous breaking of baryon number symmetry, and the identification of the D1-brane as an axionic string [24, 25, 26].

baryonic degrees of freedom.[4] The moduli space of the single D3-brane probe in this case is

$$M_{11}M_{22} - M_{12}M_{21} = \Lambda^4 \tag{2.5}$$

namely, a deformed conifold geometry. Hence the strong coupling dynamics of the field theory encodes the deformed geometry at the infrared end of the cascade, dictating the size of the finite S^3.

The general idea is that the gauge theory living on the D-brane world volume perceives the deformed geometry that becomes important at a given scale as a quantum deformation of its moduli space. This technique will generalize to more complicated cascades and infrared behaviors in the next sections.

2.2 The supergravity throats

As we discussed, the main support for the idea of a cascading RG flow for the conifold comes from the supergravity dual description [5]. In [6], analog supergravity solutions were constructed for del Pezzo surfaces. In this section we review such solutions and discuss the possibility of extending the ideas in [6] to other geometries.

These solutions are concrete examples of the Type IIB supergravity solutions introduced by Graña and Polchinski in [16] (see [28, 29] for related backgrounds in compactifications). The starting point is a warped product of four dimensional Minkowski space and a Calabi-Yau 3-fold X

$$ds^2 = Z^{-1/2}\eta_{\mu\nu}dx^\mu dx^\nu + Z^{1/2}ds_X^2 \tag{2.6}$$

with the warp factor Z depending only on internal coordinates of the Calabi-Yau. In addition there is a 3-form flux

$$G_3 = F_3 - \frac{i}{g_s}H_3 \tag{2.7}$$

It was shown in [16] that (2.6) and (2.7) lead to a solution that preserves $\mathcal{N} = 1$ supersymmetry provided that G_3 has support only on the Calabi-Yau X, is imaginary self-dual with respect to the Hodge star on X, and is a harmonic $(2, 1)$ form.

More specifically, we will be interested in cases in which the Calabi-Yau is a complex cone over a del Pezzo surface. Thus, its metric has the typical form

---

[4]A more precise statement would be to stick to the non-Abelian case, without overall $U(1)$, but study the dynamics along the generic mesonic Higgs branch. Our results below would arise for the relative $U(1)$'s controlling the relative positions of the D-branes. The trick of simplifying the discussion by restricting to the Abelian quiver theory is a standard manipulation for branes at singularities, see [27] for further discussion.

$$ds_X^2 = dr^2 + r^2\eta^2 + r^2 h_{a\bar{b}} dz^a d\bar{z}^{\bar{b}} \tag{2.8}$$

where $\eta = \left(\frac{1}{3}d\psi + \sigma\right)$ and $h_{a\bar{b}}$ denotes the Kähler-Einstein metric on the del Pezzo surface. It is important to remember that dP_n only admits Kähler-Einstein metrics for $n \geq 3$, and thus our construction will be valid in this range and will not be applicable to the first del Pezzos.[5] One however expects that gauge theory cascades for these theories exist, and presumably correspond to other throat structures (indeed the supergravity dual of a dP_1 cascade belongs to the class recently constructed in [13]).

For dP_n, $h^{2,0} = 0$ and $h^{1,1} = n + 1$. Thus, there are $n + 1$ harmonic $(1, 1)$ forms. One of them is the self-dual Kähler form ω. It is possible to pick the remaining $(1, 1)$ forms ϕ_I, $I = 1 \ldots n$, such that

$$\phi_I \wedge \omega = 0 \tag{2.9}$$

Also, these forms are anti-selfdual. With this basis at hand, it is straightforward to construct the 3-form flux

$$G_3 = \sum_{I=1}^{k} a^I (\eta + i\frac{dr}{r}) \wedge \phi_I \tag{2.10}$$

where, at this point, the a_I are constant coefficients determining the solution. It is easy to check that (2.10) satisfies all the conditions presented above and leads to a supersymmetric solution.

The warp factor in (2.6) becomes, for dP_n,

$$Z(r) = \frac{2 \cdot 3^4}{9 - n}\alpha'^2 g_s^2 \left(\frac{\ln(r/r_0)}{r^4} + \frac{1}{4r^4}\right) \sum_{i,j} M^I A_{IJ} M^J \tag{2.11}$$

The number of fractional branes M^J is measured by the integrals of the RR 3-form F_3 over the 3-cycles in the 5-dimensional base, obtained by fibering the $U(1)$ fiber over the 3-cycles dual to ϕ_I (namely, over the 3-cycles dual to $\eta \wedge \phi_I$). The solutions describe RG flows in which the number of D5-branes of each type remains constant

$$a^J = 6\pi\alpha' M^J \tag{2.12}$$

and the effective number of D3-branes runs logarithmically with the scale.

---

[5]dP_0 also admits a Kähler Einstein metric but cannot admit fractional D3-branes, due to the absence of collapsing 2-cycles, and therefore will not be considered here.

$$N = \frac{3}{2\pi} g_s \ln(r/r_0) \sum_{I,J} M^I A_{IJ} M^J, \tag{2.13}$$

with A_{IJ} the intersection matrix on dP_n.

Another remarkable fact of this supergravity dual is that it reproduces the field theory computation of n combinations of the $n + 3$ gauge coupling beta functions (corresponding to n marginal couplings in the conformal case) [6]. They are encoded in the evolution of the NSNS 2-form in the radial direction due to the non-trivial NSNS 3-form flux.

The construction of these throats is important since it illustrates that cascading RG flows appear often in quiver gauge theories. Moreover, warped throats are interesting both from the viewpoint of phenomenological applications (e.g. [29, 30, 31]) and of counting flux vacua, due to their 'attractor' behavior [33]. Our purpose in this paper is to clarify the infrared structure of these (and similar) classes of models, a key understanding required for the above applications.

These throats contain a naked singularity at their origin, and hence are the analogs of the KT throat [5] for the conifold. In later sections we will clarify that the dual gauge theory infrared dynamics suggests that in many situations a suitable deformation of the geometry eliminates the singularity, and yields a smooth supergravity solution, the analog of the solution in [2] for the conifold.

The above construction of throats was originally elucidated for the case of del Pezzo surfaces. Nevertheless, its range of applicability is much broader and it is indeed suitable for any other complex cone over a 4-dimensional surface Y^4 with a Kähler-Einstein metric. In the general case, the ϕ_I, with $I = 1 \dots h^{1,1}(Y^4) - 1$, correspond to a basis of harmonic $(1,1)$ forms chosen to be orthogonal to the Kähler form on Y^4, and A_{IJ} is a general matrix encoding the cup product among them (alternatively, the geometric information regarding the intersections between the 2-cycles in Y^4 which are Poincaré dual to the ϕ_I's). Indeed, the warped conifold belongs to the above class of solution, by considering the case of a single 2-form orthogonal to ω, and with the matrix A_{IJ} reduced to a single entry.

Finally, we would like to mention that there exist more general situations, where the conical Calabi-Yau singularity corresponds to a real cone over a Sasaki-Einstein 5-dimensional horizon X_5 as before, but X_5 cannot be constructed as a $U(1)$ fibration over a 4-dimensional Kähler-Einstein base. Simple examples of this class are provided by the complex cones over dP_1 and dP_2, where the $U(1)$ fibration over the del Pezzo surface is irregular. This fact maps, on the gauge theory side, to irrational R-charges. Moreover, recently, an infinite family of cones over 5d Sasaki-Einstein manifolds, denoted $Y^{p,q}$, with explicit metrics has been constructed [7, 8, 9, 10, 11]. Also, the dual quiver gauge theories have been found in [12].

Duality cascades for the case of $Y^{2,1}$, corresponding to the 5d horizon of a complex cone over dP_1, were constructed in [6], and duality cascades for the entire $Y^{p,q}$ family along with their supergravity duals have been recently carried out in [13]. An interesting difference with respect to the above throats is an additional dependence of the warp factor on a coordinate of the 5d horizon X_5, rather than just on the radial direction.

Finally, notice that, using our arguments in coming sections, one can show that the $Y^{p,q}$ cascades do not in general admit a geometric deformation to resolve their singularities. The only cases where this is possible correspond to cones over $Y^{p,0}$, which are in fact $\mathbb{Z}_p$ quotients of the conifold. They thus fall within our analysis, and we describe the field theory version of their smoothing in Appendix C.

2.3 The deformed geometries

The above throats contain a naked singularity, suggesting that they miss the non-perturbative infrared dynamics of the dual gauge field theory. Hence they are the analogs of the singular solution in [5]. From the discussion of the conifold it is expected that, at least in some cases, when the infrared gauge theory dynamics is included, the dual supergravity solution corresponds to a deformed background related to the original one by an extremal transition. This transition replaces 2- and 4-cycles by 3-cycles. A general question is therefore to analyze the existence of extremal transitions on local Calabi-Yau geometries, where shrinking 4-cycles are replaced by finite size 3-cycles.

In this section we address this geometric question from several viewpoints. For concreteness we center the discussion on the geometries given by complex cones over del Pezzo surfaces, although results generalize to other situations, as will be clear in our examples.

The general question is what are the possible deformations of the complex cones over del Pezzo surfaces. Besides its relevance to the above discussion, this question has another interesting realization. Geometries with collapsing del Pezzo surfaces lead, when used as M-theory backgrounds, to five-dimensional field theories with E_n global symmetries. The Coulomb branch is parametrized by the sizes of the 2-cycles, while the Higgs branch corresponds to extremal transitions, i.e. complex deformations of the geometry arising at the origin of the Coulomb branch, where the 4-cycle shrinks to zero size. The classification of such Higgs branches was described in [34], and shown [35] to fully agree with the geometric description.[6]

---

[6] A concise description of these Higgs branches is provided by the instanton moduli space of the corresponding E_n gauge theory. The relation is manifest by realizing the five-dimensional field theory in the worldvolume of D4-branes probing configurations of D8-branes/O8-planes at strong coupling, so that the

In many examples, one may use the realization of the five-dimensional field theories in terms of (p, q) webs of Type IIB fivebranes [21, 22], in order to visualize the corresponding Higgs branches. This corresponds to the situations where the geometries are toric, and the (p, q) web corresponds to the reciprocal of the collection of points in the $\mathbb{Z}^2$ integer lattice defining the toric diagram [22, 23]. In general, for toric geometries with a corresponding web, deformations exist if there are subsets of external legs which can form sub-webs in equilibrium. The deformation is described as the separation of such sub-webs. A more precise description of this in toric geometry language is illustrated in some examples in Appendix B.

The (p, q) web representation of the deformation for the conifold is described in Figure 1, where the sub-webs correspond to straight lines. The 3-cycle in the deformed conifold corresponds to a segment stretched between the two sub-webs. For example in 5 dimensional gauge theories a D3-brane stretched between the two (p, q) sub-webs is a BPS brane on the Higgs branch, which maps to a brane wrapped on the 3-cycle in the geometry.

Using the toric diagrams for the cones over del Pezzo surfaces one can recover the results in [35]. Namely, for dP_0 and dP_1 there is no deformation branch, as is manifest from their toric pictures, Figure 2.
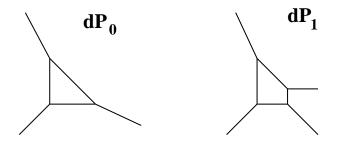

Figure 2: Web diagrams for the complex cones over dP_0 and dP_1. In both cases, it is impossible to split them into more than one sub-webs in equilibrium, implying there exist no complex deformations for these geometries.

On the other hand, dP_2 has a deformation, shown in Figure 3, which completely smoothes out the geometry. For dP_3 there are two deformation branches, one of them two-dimensional and the other one-dimensional, see Figure 4. Notice that the two-dimensional deformation branch may be regarded as a one-dimensional deformation to the conifold, subsequently followed by a one-dimensional deformation to a smooth space. This is more manifest in the regime of widely different sizes for the two independent 3-cycles.

global symmetry is enhanced to E_n [34]. The Higgs branch corresponds to dissolving the D4-brane as an instanton of the E_n gauge theory.
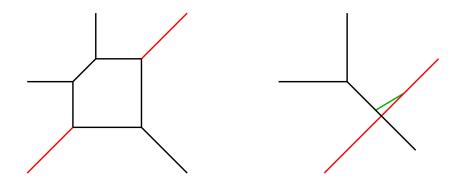
Figure 3: The web diagram for the complex cone over dP_2 and its complex deformation.
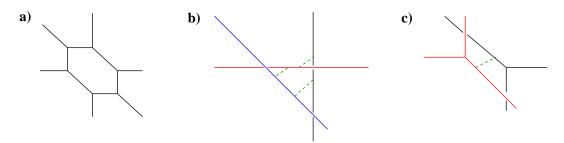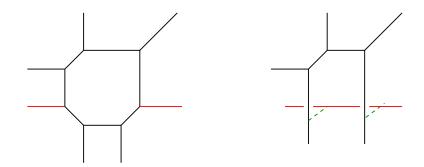

Figure 4: Web diagram for the complex cone over dP_3 and its two branches of complex deformation. Figure b) shows a two-dimensional deformation branch, parametrized by the sizes of two independent 3-spheres corresponding to the dashed segments (the three segments are related by a homology relation, hence only two are independent). Figure c) shows a one-dimensional deformation branch.

For higher del Pezzo surfaces, the generic geometry is not toric. However, there are closely related blow-ups of $\mathbb{P}_2$ at non-generic points, which do admit a toric description. These non-generic geometries lead to the same quivers than the del Pezzos, but with different superpotentials. For non-toric del Pezzos, some deformations are manifest in the toric representation, see Figure 5 for an example. Notice however that the dimensions of these deformation branches is in general lower than that for generic geometries, thus showing that some deformations of the higher del Pezzos are non-toric.

In a similar spirit, we may consider other toric geometries closely related to toric del Pezzos, but corresponding to a non-generic location of the blow-ups.[7] They are given by web diagrams associated to the so-called less symmetric quiver gauge theories. For such

---

[7]Here the distinction between toric and quiver webs is relevant [36]. In these cases, the web diagram corresponds to the quiver web, and encodes the quiver data of a less symmetric phase of the gauge theory. On the other hand, the geometry is still described by some toric data, corresponding to a toric web, different in general from the quiver web. See [36] for a detailed discussion.

Figure 5: Web diagram for a cone over a non-generic blow-up of $\mathbb{P}^2$ at four points and its deformation. This geometry is toric and is closely related to dP_4. The two dashed segments correspond to two homologically equivalent 3-spheres. The left-over diagram describes a suspended pinch point singularity, which admits a further deformation not shown in the picture.

geometries, deformations to smooth geometries exist, although the generic deformation may not be available. One example of a deformation on a non-generic version of dP_3 is shown in Figure 6.

Figure 6: Web diagram for the cone over a non-generic dP_3 and its deformation to the orbifold $\mathbb{C}^3/\mathbb{Z}_2$.

Finally, we emphasize that the above techniques can be used to study the deformations of other geometries, even involving more than one collapsing 4-cycles. Concrete examples, like the deformations of the cone over F_0, the suspended pinch point singularity and the $Y^{p,q}$ geometries will appear in subsequent sections. It is interesting to point out that all possible complex deformations for toric varieties may not be described using the above web deformations. Nevertheless, all our examples will be of this kind. We leave the interesting question of other possible situations for future research.

2.4 A topological consideration

The throats on cones over dP_n constructed in [6] (and generalizations) have in principle n independent discrete parameters, the M^I, associated to the integer fluxes sourced by the n independent fractional branes one can in principle introduce in the quiver gauge theory.

However, in this section we describe a topological argument which shows that in order for a throat to have a smooth deformation at its bottom, corresponding to a geometric deformation as discussed above, the fractional brane assignments cannot be fully arbitrary. Equivalently, it is possible to use topological information about the allowed deformations to derive the set of fractional branes triggering the corresponding strong infrared dynamics.

The argument is as follows. The fractional brane numbers can be measured in the throat solution by computing the flux of the RR 3-form F_3 through a 3-cycle in the 5d base of the cone (constructed as an S^1 fibration over a 2-cycle in the del Pezzo surface [8]). There are n such 3-cycles. On the other hand, in the smooth deformed geometries, one in general finds a smaller number k of 3-cycles. This implies that $n - k$ 3-cycles in the asymptotic region are homologically trivial. Consequently, only k independent choices of fractional brane numbers remain.

For each deformed geometry, the set of corresponding fractional branes, i.e. those associated to the homologically non-trivial 3-cycles, is determined as follows. Consider a given complex deformation, corresponding to the separation of sub-webs. Recall now the relation between external legs in web diagram and nodes in the quiver [37, 38]. The fractional branes associated to the deformation are those controlling the rank of the nodes corresponding to the legs in the removed sub-web. We will see some examples of this in later sections.

Notice that this does not mean there are no throat solutions for more general fractional brane assignments, but rather that they cannot be completed in terms of a purely geometric background. The most plausible proposal is that the general case corresponds to a smooth deformed geometry (accounting for the fractional branes associated to non-trivial 3-cycles) with additional explicit fractional brane sources, leading to a non-trivial dF_3, which induces a non-vanishing F_3 flux at large radial distances for the homologically trivial 3-cycles.

2.5 Deformations from the gauge theory

In the previous sections, we have introduced the simple example of the conifold and discussed how the original naked singularity in the supergravity dual is cured when the strong coupling

---

[8]Although we focus on the case of del Pezzo surfaces, the discussion applies to other real four dimensional Kähler-Einstein surfaces.

dynamics of the gauge theory is taken into account. We then reviewed how more general extremal transitions are described using toric geometry in the form of (p, q) webs.

We now describe the derivation of the geometric deformation from the viewpoint of the infrared dynamics of the dual gauge theory, for a general quiver theory. As in the conifold case above, the deformation can be derived as the deformed moduli space of probes, arising from the quantum modification of the moduli space of the gauge theory. Although the basic idea follows discussions in [2], its implementation in our more involved geometries leads to richer structures.

The geometries we study have several collapsing 2-cycles on which we can wrap D5-branes, giving rise to different types of fractional branes. In order for the supergravity solutions described in Section 2.2 to be valid we will assume that the number of fractional branes of each type $M^I \ll N$. There is no constraint on the relative sizes of the M^I's. However, in order to simplify our discussion, we can consider the situation in which

$$M^1 \ll M^2 \ll \ldots \ll \ldots \ll N \tag{2.14}$$

Then it is natural to foresee a hierarchy of scales of strong gauge dynamics

$$\Lambda_1 \ll \Lambda_2 \ll \ldots \ll \Lambda_3 \tag{2.15}$$

where the Λ_I's are dynamical scales that arise when $N(\Lambda_I)$ is comparable to M_I

$$\Lambda_I \text{ such that } N(\Lambda_I) \sim M^I \tag{2.16}$$

We have simplified the field theory analysis by assuming the scales are well separated, although we expect that descriptions of other situations exist in both the smooth supergravity solution and the gauge theory language.

The basic structure of strong infrared dynamics is the following. Given a quiver gauge theory with fractional branes, the theory cascades down until the number of D3-branes N becomes similar to one of the fractional brane numbers, say M^{I_0}, at a scale Λ_{I_0}. For simplicity, and due to our assumption of separation of scales, we may ignore the remaining M^I's and take them to vanish. In order to simplify notation, we call $M^{I_0} = M$. Then the last step of the cascade can be probed by introducing M additional D3-branes and studying the resulting moduli space. In this situation the gauge group takes the form

$$SU(2M)^m \times SU(M)^n \tag{2.17}$$

In several of our examples below, the number of gauge factors with rank $2M$ is two [9], $m = 2$, but the discussion may be carried out in general. Also, in the explicit models the number of flavors for the $SU(2M)$ gauge factors is $2M$, hence equals the number of colors.

The non-perturbative dynamics may be determined by assuming, to begin with, that the $SU(M)$ gauge factors are weakly coupled and act as spectators, corresponding to global flavor symmetries. For simplicity we continue the discussion assuming also that there no arrows among $SU(2M)$ nodes, i.e. no $(2M, \overline{2M})$ matter. Under these circumstances, the strong dynamics corresponds to a set of decoupled $SU(2M)$ gauge theories with equal number of colors and flavors, which thus develop a non-perturbative *quantum modification of the moduli space*. This is best understood in terms of gauge invariant mesonic and baryonic variables. For each such gauge factor, the mesons are

$$\mathcal{M}_{ru} = A_r B_u \tag{2.18}$$

with $r, u = 1, 2$, where

$$A_r : (2M, \overline{M}_r) \qquad B_u : (M_u, \overline{2M}) \tag{2.19}$$

and the baryons have the abbreviated form

$$\mathcal{B} = [A]^{2M} \qquad \tilde{\mathcal{B}} = [B]^{2M} \tag{2.20}$$

where antisymmetrization of gauge indices is understood. It is important to keep in mind that these operators are not gauge invariant when the entire gauge group (and not just the factors undergoing deformation) is taken into account. This will be important when we study what happens after they develop non-zero vevs. The quantum modified moduli space is described by

$$\det \mathcal{M} - \mathcal{B}\tilde{\mathcal{B}} = \Lambda^{4M} \tag{2.21}$$

The resulting infrared gauge dynamics is described by a quiver gauge theory with the $SU(2M)$ nodes removed, the corresponding flavors replaced by mesonic and baryonic degrees of freedom (both in the quiver diagram and in the superpotential), and with the quantum modified constraints enforced as superpotential interactions by means of singlet chiral field Lagrange multipliers X, of the form[10]

---

[9]In the (p, q) web description of the deformations presented in Section 2.3, this arises naturally when one of the sub-webs that are separated is simply an infinite straight line.

[10]For simplicity, we show only one Lagrange multiplier and additional superpotential term. It us understood that there is one such contribution for each strongly coupled gauge group factor.

$$W = W_0 + X(\det \mathcal{M} - \mathcal{B}\tilde{\mathcal{B}} - \Lambda^{4M}) \tag{2.22}$$

The quantum constraints force some of the meson/baryon degrees of freedom to acquire non-zero vevs. The dynamics of the probes is recovered along the mesonic branch, which corresponds to setting the baryons to zero and $X = \pm\Lambda^{4-4M}$, and saturating the constraint with meson vevs (see footnote 3). This triggers symmetry breaking of some of the $SU(M)$ factors to diagonal combinations, and makes some of the fields massive due to superpotential couplings. The resulting theory contains a set of meson fields with quantum deformed moduli space, describing the probes in the deformed geometry. In addition, there are additional gauge factors and chiral multiplets describing the geometry left-over after the complex structure deformation of the original one. In later sections we will present several examples, in which the matching between the gauge theory description of the quantum deformations and the geometric complex structure deformations is complete. This is a very satisfactory result.

There is a subtlety in fixing the sign of the vev for X. The simplest way of determining the correct one is to impose that, restricting to the Abelian case, the theory has a superpotential allowing for a toric description of its moduli space. Concretely, that each bi-fundamental field appears with opposite signs in the two terms containing it. This recipe can be recovered from a more careful treatment of the equation of motion determining X from the initial superpotential, as discussed in a concrete example in Appendix A.

After the condensation, the left-over quiver theory may correspond to a singular geometry with fractional branes, and thus will have subsequent duality cascades and condensations. The resulting RG flow takes in this case the form of a cascade with multiple dynamical scales at which the underlying geometry undergoes deformation. Explicit examples are discussed in coming sections.

3. Some warmup examples

In this section we would like to describe some simple examples of infrared resolutions, in situations with one-scale cascades.

3.1 The cone over F_0

Let us consider the case of the cone over F_0. The web diagram for this geometry is shown in Figure 7a, and the corresponding quiver is in Figure 8a.
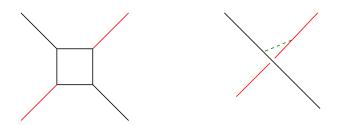
Figure 7: Web diagram for the complex cone over F_0, and its complex deformation to a smooth space.
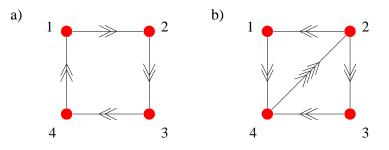

Figure 8: Figure a) shows the quiver diagram for the theory of D3-branes at a complex cone over F_0. Figure b) shows a dual phase of the theory, involved in the duality cascade.

The fractional brane corresponds to the rank vector $(0, 1, 0, 1)$. The superpotential for the theory is

$$W = X_{12}X_{23}Y_{34}Y_{41} - X_{12}Y_{23}Y_{34}X_{41} - Y_{12}X_{23}X_{34}Y_{41} + Y_{12}Y_{23}X_{34}X_{41} \qquad (3.1)$$

in self-explanatory notation. This theory has an $SU(2) \times SU(2)$ global symmetry, which geometrically arises as the product of the $SU(2)$ isometries of the two $\mathbb{P}^1$'s in $F_0 = \mathbb{P}^1 \times \mathbb{P}^1$. It corresponds to a $\mathbb{Z}_2$ orbifold of the conifold $xy - zw = 0$ by the action $x, y, z, w \rightarrow -x, -y, -z, -w$, as first determined in [27]. This is also manifest in the dual toric diagrams, where the cone over F_0 differs from the conifold by the addition of an interior point (namely, by the refinement of the toric lattice).

This theory has a cascade, which was exhaustively discussed in [4, 6], to which we refer the reader for details. Introducing N D3-branes and M fractional branes, namely starting quiver 8a with the rank vector

$$N(1, 1, 1, 1) + M(0, 1, 0, 1) \qquad (3.2)$$

the theory alternates between the two quivers in Figure 8a, b. Given the $\mathbb{Z}_2$ symmetry of the quiver and of the deformed geometry, it is natural to consider the situation where the UV gauge couplings of opposite nodes are equal. In this case, the duality cycle is obtained by

a (simultaneous) dualization of the nodes 1 and 3, followed by a (simultaneous) dualization of 2 and 4, after which 1 and 3 are subsequently dualized, etc. Under these conditions, quiver 8b appears just as an intermediate step between simultaneous dualizations. In each duality cycle, the number of D3-branes decreases by $2M$ units. It is interesting to note that, regarding the geometry as a quotient of the conifold, nodes 1 and 3 descend from a single node in the quiver of the conifold, while 2 and 4 descend from the other. In this respect, the duality cascade in the orbifold theory, in the situation of symmetric gauge couplings for opposite nodes in the quiver, can be regarded as directly descending from the duality cascade in the conifold theory.

The infrared end of the cascade is therefore expected to be similar to that of the conifold. In fact, this is exactly what is obtained e.g. for N a multiple of M. The gauge theory associated to the rank vector $(0, M, 0, M)$, leads to two decoupled $\mathcal{N} = 1$ SYM-like theories. In more detail, the infrared behavior may be explored by introducing M additional D3-brane probes, namely by studying the gauge theory with rank vector $(M, 2M, M, 2M)$. In the infrared the gauge factors 1 and 3 are weakly coupled, and can be considered spectators. The gauge factors 2 and 4 have $N_f = N_c$ and develop a quantum deformation of their moduli space. Following the general discussion in Section 2.5, we introduce the mesons

$$\mathcal{M} = \begin{bmatrix} M_{11} & M_{12} \\ M_{21} & M_{22} \end{bmatrix} = \begin{bmatrix} X_{12}X_{23} & X_{12}Y_{23} \\ Y_{12}X_{23} & Y_{12}Y_{23} \end{bmatrix} \quad ; \quad \mathcal{N} = \begin{bmatrix} N_{11} & N_{12} \\ N_{21} & N_{22} \end{bmatrix} = \begin{bmatrix} X_{34}X_{41} & X_{34}Y_{41} \\ Y_{34}X_{41} & Y_{34}Y_{41} \end{bmatrix}$$

and the baryons $\mathcal{B}, \tilde{\mathcal{B}}, \mathcal{C}, \tilde{\mathcal{C}}$

The quantum modified superpotential reads

$$W = M_{11}N_{22} - M_{12}N_{21} - M_{21}N_{12} + M_{22}N_{11} +$$
$$+ X_1 \left(\det \mathcal{M} - \mathcal{B}\tilde{\mathcal{B}} - \Lambda^{4M} \right) + X_2 \left(\det \mathcal{N} - \mathcal{C}\tilde{\mathcal{C}} - \Lambda^{4M} \right) \tag{3.3}$$

where we have introduced a single strong coupling scale due to the equality of the gauge couplings along the flow.

In order to study the mesonic branch, we have

$$X_1 = \Lambda^{4-4M} \quad ; \quad \mathcal{B} = \tilde{\mathcal{B}} = 0 \quad ; \quad X_2 = \Lambda^{4-4M} \quad ; \quad \mathcal{C} = \tilde{\mathcal{C}} = 0$$
$$\det \mathcal{M} = \Lambda^{4M} \quad ; \quad \det \mathcal{N} = \Lambda^{4M} \tag{3.4}$$

Now restricting to the Abelian case (see footnote 4), the resulting superpotential is

$$W = M_{11}N_{22} - M_{12}N_{21} - M_{21}N_{12} + M_{22}N_{11} - M_{11}M_{22} + M_{12}M_{21} - N_{11}N_{22} + N_{12}N_{21}$$

That is, the superpotential becomes entirely quadratic. The gauge group is broken to the diagonal combination of nodes 1 and 3 by the expectation values of the mesons. Using the equations of motion, the superpotential vanishes. The only degrees of freedom are one set of mesons, due to the equations of motion, which require $\mathcal{M} = \mathcal{N}$. In addition, these mesons are subject to the quantum constraints, namely $\det \mathcal{M} = \Lambda^4$. This describes the dynamics of the probes in the deformation of the cone over F_0 to a smooth space. Indeed, at any point in the mesonic branch (in the Abelian case) the gauge group is $U(1)$ and there are three adjoint (i.e. uncharged) chiral multiplets with vanishing superpotential. This is the $\mathcal{N} = 4$ $U(1)$ SYM of D3-branes probing a smooth space.

The analogy of the above discussion with the conifold case is manifest from the orbifold description. Moreover, from the geometric viewpoint the deformation of the cone over F_0 corresponds simply to the quotient of the deformed conifold $xy - zw = \epsilon$ by the $\mathbb{Z}_2$ action $x, y, z, w \to -x, -y, -z, -w$, under which it is invariant.

The complex cone over F_0 is one of the first examples in the family of real cones over the manifolds $Y^{p,0}$ introduced in [7, 8, 9, 10, 11], namely $Y^{2,0}$. The real cones over $Y^{p,0}$ correspond to quotients of the conifold $xy - zw = 0$ by the $\mathbb{Z}_p$ action generated by

$$ x \to e^{2\pi i/p} x \quad , \quad y \to e^{-2\pi i/p} y \quad , \quad z \to e^{2\pi i/p} z \quad , \quad w \to e^{-2\pi i/p} w \tag{3.5} $$
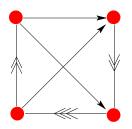
(with $Y^{1,0}$ corresponding to $T^{1,1}$, the base of the conifold itself). This orbifold action is easily understood by looking at the toric diagrams for these varieties. The toric diagrams look like the diagram of the conifold with an additional refinement of the lattice.

Moreover, using the web diagrams for these varieties it follows that these are the only examples of cones over the manifolds $Y^{p,q}$ which admit a complex deformation which smoothes the singularity. Namely, only for the case of $q = 0$ we expect that complex deformations will smooth out the naked singularity at the tip of the warped throat solutions in the presence of fluxes as in [13]. The discussion of the geometries involved and the field theory description of the smoothing is presented in Appendix C.

3.2 First del Pezzos

Let us consider the cones over the first del Pezzo surfaces. As already mentioned, the cone over dP_0 does not admit any fractional branes, and therefore cannot be taken away from the conformal regime.

The quiver diagram for a cone over dP_1 is presented in Figure 9. The corresponding superpotential is

Figure 9: Quiver diagram for D3-branes at the cone over dP_1.

$$W = \epsilon_{\alpha\beta}X_{34}^\alpha X_{41}^\beta X_{13} - \epsilon_{\alpha\beta}X_{34}^\alpha X_{42}X_{23}^\beta + \epsilon_{\alpha\beta}X^{12}X_{34}^3 X_{41}^\alpha X_{23}^\beta \qquad (3.6)$$

This theory admits one kind of fractional branes, given by the rank vector $(0, 3, 1, 2)$. The addition of these fractional branes leads to an RG cascade which was first studied in [6]. The superpotential (3.6) preserves an $SU(2) \times U(1)$ global symmetry. The R-charges can then be determined using the a-maximization principle, and turn out to be irrational numbers [11]. Some explicit computations can be found in [14]. This is the simplest example of a singularity whose dual gauge theory has irrational R-charges. Thus, it is very interesting to understand the associated cascades in detail and we now proceed to do so.

The resulting RG flow is logarithmic and periodic. For an appropriate choice of initial couplings, the sequence of dualized nodes in a period is 2, 4, 3, 1, after which $N \to N - 4M$ and M. The quivers for several steps in the cascade are shown in Figure 10.

The beta functions at each step are

	N_1	N_2	N_3	N_4	β_1/M	β_2/M	β_3/M	β_4/M
1	N	$N+3M$	$N+M$	$N+2M$	$-10+\sqrt{13}$	$\mathbf{10-\sqrt{13}}$	$22-7\sqrt{13}$	$-22+7\sqrt{13}$
2	N	$N-M$	$N+M$	$N+2M$	$22-7\sqrt{13}$	$-10+\sqrt{13}$	$-22+7\sqrt{13}$	$\mathbf{10-\sqrt{13}}$
3	N	$N-M$	$N+M$	$N-2M$	$-22+7\sqrt{13}$	$22-7\sqrt{13}$	$\mathbf{10-\sqrt{13}}$	$-10+\sqrt{13}$
4	N	$N-M$	$N-3M$	$N-2M$	$\mathbf{10-\sqrt{13}}$	$-22+7\sqrt{13}$	$-10+\sqrt{13}$	$22-7\sqrt{13}$
5	N	$N-4M$	$N-3M$	$N-2M$	$-10+\sqrt{13}$	$\mathbf{10-\sqrt{13}}$	$22-7\sqrt{13}$	$-22+7\sqrt{13}$

$$(3.7)$$

where we have indicated the beta functions of the dualized nodes with a bold font.

In addition, the supergravity dual of this flow corresponds to the $Y^{2,1}$ flow, which is a member of the class of warped throat solutions recently constructed in [13]. However, as already mentioned, the geometry does not admit a complex deformation, hence the naked singularity at the infrared is not removed by this mechanism. This remains an open question we hope to address in the future.

The first non-trivial example of complex deformation is provided by the cone over dP_2. The web diagram is shown in Figure 3a, and the corresponding quiver diagram is in Figure
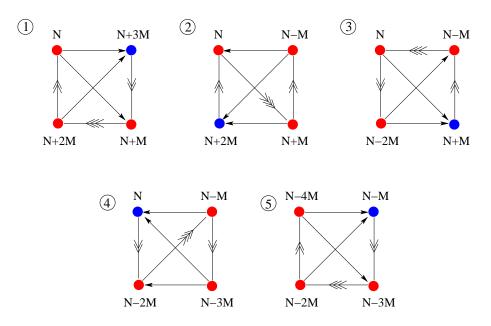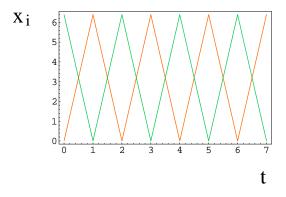
Figure 10: Quivers in a duality cycle in the duality cascade of dP_1. We have indicated in blue the dualized node at each step.

Figure 11: Evolution of the inverse squared couplings $x_i = 8\pi^2/g_i^2$ as a function of $t = \log\mu$ for the dP_1 cascade under consideration. UV couplings have been chosen respecting the quiver symmetries and such that the sequence given by Figure 10 and (3.7) is followed. We indicate x_1 and x_2 in green, and x_3 and x_4 in orange.

12.

The superpotential for this theory is given by

$$W = X_{34}X_{45}X_{53} - (X_{53}Y_{31}X_{15} + X_{34}X_{42}Y_{23})$$
$$+ (Y_{23}X_{31}X_{15}X_{52} + X_{42}X_{23}Y_{31}X_{14}) - X_{23}X_{31}X_{14}X_{45}X_{52} \tag{3.8}$$

The two independent fractional branes can be taken to correspond to the rank vectors $(1, 1, 0, 0, 0)$ and $(0, 1, 0, 1, -1)$. The existence of an RG cascade in this theory, although
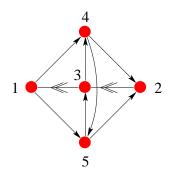
Figure 12: Quiver diagram for D3-branes at the cone over dP_2.

expected, has not been established in the literature, neither from the field theory nor the supergravity viewpoint.

Using our arguments in section 2.4, it is possible to see that the cascade ending in the deformation shown in figure 3a corresponds to the first type of fractional branes. We thus proceed to study it, taking initial ranks of the form

$$\vec{N} = N(1, 1, 1, 1, 1) + M(1, 1, 0, 0, 0) \tag{3.9}$$

We will consider UV couplings respecting the $\mathbb{Z}_2$ symmetry that the quiver has in the absence of fractional branes, $x_1 = x_2$ and $x_4 = x_5$.
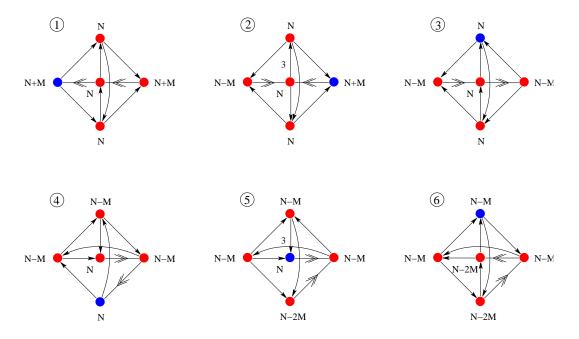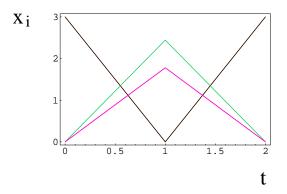

Figure 13: Some quivers in a duality cycle in the duality cascade of dP_2. We have indicated in blue the dualized node at each step.

The sequence of gauge group ranks and beta functions for the gauge couplings is

	N_1	N_2	N_3	N_4	N_5	β_1/M	β_2/M	β_3/M	β_4/M	β_5/M
1	$N+M$	$N+M$	N	N	N	**3**	3	$\frac{3}{4}(-9+\sqrt{33})$	$\frac{3}{8}(1-\sqrt{33})$	$\frac{3}{8}(1-\sqrt{33})$
2	$N-M$	$N+M$	N	N	N	-3	**3**	0	0	0
3	$N-M$	$N-M$	N	N	N	-3	-3	$\frac{3}{4}(9-\sqrt{33})$	$\frac{\mathbf{3}}{\mathbf{8}}(\mathbf{-1}+\sqrt{\mathbf{33}})$	$\frac{3}{8}(-1+\sqrt{33})$
4	$N-M$	$N-M$	N	$N-M$	N	$\frac{3}{8}(1-\sqrt{33})$	$\frac{3}{4}(-9+\sqrt{33})$	3	$\frac{3}{8}(1-\sqrt{33})$	**3**
5	$N-M$	$N-M$	N	$N-M$	$N-2M$	0	0	**3**	0	-3
6	$N-M$	$N-M$	$N-2M$	$N-M$	$N-2M$	$\frac{3}{8}(-1+\sqrt{33})$	$\frac{3}{4}(9-\sqrt{33})$	-3	$\frac{\mathbf{3}}{\mathbf{8}}(\mathbf{-1}+\sqrt{\mathbf{33}})$	-3

$$(3.10)$$

Figure 14: Evolution of the inverse squared couplings $x_i = 8\pi^2/g_i^2$ as a function of $t = \log\mu$ for some steps in the dP_2 cascade under consideration. UV couplings have been chosen respecting the quiver symmetries and such that the sequence given by Figure 13 and (3.10) is followed. We indicate x_1 and x_2 in black, x_3 in green, and x_4 and x_5 in magenta.

Figure 14 shows a typical evolution of gauge couplings in this case. For simplicity, Figure 13 and (3.10) only show six steps in the duality cascade. At the end of this pattern of dualization, one obtains a quiver similar to the original one, up to a reduction of the number of D3-branes and a rotation of the diagram. Hence continuation of this pattern eventually leads to a full duality cycle, and thus a periodic cascade.

Let us now explore the behavior of the theory for small number of regular D3-branes, which corresponds to the infrared of the RG cascade. For that, we consider M D3-branes probing the theory at the IR end of the cascade. Hence, let us consider the gauge theory described by the rank vector

$$\vec{N} = M(1,1,1,1,1) + M(1,1,0,0,0) \tag{3.11}$$

In this situation the nodes 1 and 2 have $N_f = N_c$ and develop a quantum deformed moduli space. The meson fields for nodes 1 and 2 are

$$\mathcal{M} = \begin{bmatrix} M_{34} & M_{35} \\ \tilde{M}_{34} & \tilde{M}_{35} \end{bmatrix} = \begin{bmatrix} X_{31}X_{14} & X_{31}X_{15} \\ Y_{31}X_{14} & Y_{31}X_{15} \end{bmatrix} \quad ; \quad \mathcal{N} = \begin{bmatrix} N_{43} & N_{53} \\ \tilde{N}_{43} & \tilde{N}_{53} \end{bmatrix} = \begin{bmatrix} X_{42}X_{23} & X_{52}X_{23} \\ X_{42}Y_{23} & X_{52}Y_{23} \end{bmatrix}$$

The quantum modified superpotential becomes

$$\begin{aligned} W = X_{34}X_{45}X_{53} &- (X_{53}Y_{31}X_{15} + X_{34}X_{42}Y_{23}) \\ &+ (Y_{23}X_{31}X_{15}X_{52} + X_{42}X_{23}Y_{31}X_{14}) - X_{23}X_{31}X_{14}X_{45}X_{52} \\ &+ X_1 \left(\det \mathcal{M} - \mathcal{B}\tilde{\mathcal{B}} - \Lambda^{4M} \right) + X_2 \left(\det \mathcal{N} - \mathcal{C}\tilde{\mathcal{C}} - \Lambda^{4M} \right) \end{aligned} \quad (3.12)$$

Along the mesonic branch we have

$$X_1 = \Lambda^{4-4M} \quad ; \quad \mathcal{B} = \tilde{\mathcal{B}} = 0 \quad ; \quad X_2 = -\Lambda^{4-4M} \quad ; \quad \mathcal{C} = \tilde{\mathcal{C}} = 0$$
$$\det \mathcal{M} = \Lambda^{4M} \quad ; \quad \det \mathcal{N} = \Lambda^{4M} \quad (3.13)$$

The appropriate signs for the vevs for X_1 and X_2 can be determined with a reasoning identical to the one in Appendix A.

The expectation values for the mesons higgs the gauge group to a single diagonal combination of the nodes 3, 4 and 5. Restricting to the Abelian case, the superpotential becomes

$$\begin{aligned} W = X_{34}X_{45}X_{53} &- N_{53}M_{34}X_{45} - X_{53}\tilde{M}_{35} - X_{34}\tilde{N}_{43} \\ &+ \tilde{N}_{53}M_{35} + N_{43}\tilde{M}_{34} + M_{34}\tilde{M}_{35} - \tilde{M}_{34}M_{35} - N_{43}\tilde{N}_{53} + \tilde{N}_{43}N_{53} \end{aligned} \quad (3.14)$$

Using the equations of motion for e.g. $\tilde{M}_{34}$, $\tilde{M}_{35}$ and $\tilde{N}_{43}$, we have

$$M_{34} = X_{53} \quad , \quad M_{35} = N_{43} \quad , \quad X_{33} = N_{53} \quad (3.15)$$

Plugging this into (3.14) we have

$$W = X_{34}X_{45}X_{53} - X_{34}X_{53}X_{45} \quad (3.16)$$

Renaming $X_{34} = X$, $X_{45} = Y$ and $X_{53} = Z$, we obtain the $\mathcal{N} = 4$ field content and superpotential

$$W = X[Y, Z] \quad (3.17)$$

which in any event vanishes in the Abelian case, but is crucial in non-Abelian situations. Hence, the moduli space of the D3-brane probes is given by the complex deformation of the cone over dP_2 to a smooth space, as expected from the geometrical analysis.

3.3 The suspended pinch point

To illustrate that the ideas of cascades and infrared deformations are very general, we would like to consider a further example, based on the suspended pinch point (SPP) singularity. The web diagram for this geometry is shown in Figure 15a, while its deformation is in Figure 15b.
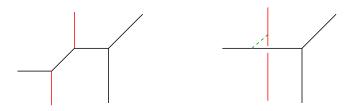

Figure 15: Web diagram for the SPP and its deformation to a smooth geometry.

The quiver diagram was determined in [27, 39] and is shown in Figure 16a, and the superpotential is

$$W = X_{21}X_{12}X_{23}X_{32} - X_{32}X_{23}X_{31}X_{13} + X_{13}X_{31}X_{11} - X_{12}X_{21}X_{11} \tag{3.18}$$

The ranks of the gauge factors are arbitrary, hence there are two independent fractional branes, which can be taken to be $(0, 1, 0)$ and $(0, 0, 1)$.
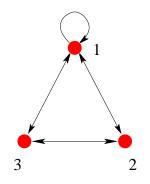

Figure 16: Quiver diagram for SPP.

Although it has not been described in the literature, the theory has a very nice and simple sequence of dualities, which as we show ends in the deformed geometry shown in Figure 15a. Similarly to what happens in the flows considered for dP_1 and dP_2, this sequence of dualities shares a very special feature with the conifold cascade: it is periodic and involves a single quiver. Let us consider the starting point given by the ranks

$$\vec{N} = N(1, 1, 1) + M(0, 1, 0) \tag{3.19}$$

27

A period in the duality sequence involves the following set of consecutive dualizations $(2, 1, 3, 2, 1, 3)$. After six dualizations, the quiver comes back to itself, with $N \to N - 3M$ and M constant. The quiver theories at each step of this sequence are shown in Figure 17. As before, we have indicated in blue the node that gets dualized at each step.
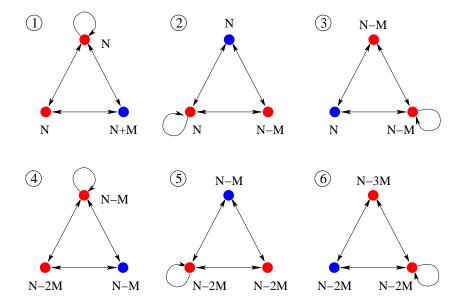

Figure 17: Sequence of quivers in one period of the SPP cascade. We have indicated in blue the dualized node at each step.

Computing the beta functions for the gauge couplings, it appears that the simple sequence in Figure 17 cannot be realized by a cascade. In particular, it is not possible to prevent a node with an adjoint from going to infinite coupling at some point in the RG flow. It would be interesting to understand whether the simple features of Figure 17 can be preserved by some more general RG flow.

When the effective number of D3-branes is comparable to M, we expect the gauge theory strong dynamics to take over and induce a geometric transition. Indeed, the SPP singularity admits a complex deformation, shown in Figure 15b. In the following we describe how this arises in the field theory.

In order to study the infrared end of the cascade, we study the gauge theory describing M D3-branes probing it. This corresponds to the quiver theory with rank vector

$$\vec{N} = M(1, 1, 1) + M(0, 1, 0) \tag{3.20}$$

In this case, we only need to consider mesons and baryons for node 2. The mesons are

given by

$$\mathcal{M} = \begin{bmatrix} M_{13} & M_{11} \\ M_{33} & M_{31} \end{bmatrix} = \begin{bmatrix} X_{12}X_{23} & X_{12}X_{21} \\ X_{32}X_{23} & X_{32}X_{21} \end{bmatrix} \tag{3.21}$$

We now introduce the quantum constraint in the superpotential and choose the mesonic branch

$$X = \Lambda^{4-4M} \quad ; \quad \mathcal{B} = \tilde{\mathcal{B}} = 0 \tag{3.22}$$

Restricting to the Abelian case, the superpotential reads

$$W = -M_{33}X_{31}X_{13} + X_{13}X_{31}X_{11} - M_{11}X_{11} + M_{33}M_{11} \tag{3.23}$$

The equation of motion for M_{11} requires $X_{11} = M_{33}$, so we get

$$W = -M_{33}X_{31}X_{13} + X_{13}X_{31}M_{33} \tag{3.24}$$

The gauge group is $SU(M)$ (due to the breaking by meson vevs $M \propto \mathbf{1}$). All three fields transform in the adjoint representation (a singlet in the Abelian case). The above theory clearly describes the field content and superpotential of $\mathcal{N} = 4$ SYM, i.e. the theory describing the smooth geometry left over after the deformation.

In addition, there remain some additional light fields, namely M_{11}, M_{13}, M_{31}, M_{33}, subject to the constraint

$$M_{13}M_{31} - M_{33}M_{11} = \Lambda^4 \tag{3.25}$$

The dynamics is that of probe D3-branes in the geometry corresponding to the deformation of the SPP to flat space. This matches nicely the geometric expectation, from the web diagrams in Figure 15, from which we see that the result of the deformation is a smooth geometry.

The relation between the field theory and the more geometrical description of the deformation can be done also using the toric geometry language. Using the construction of the moduli space of the SPP in terms of toric data (the forward algorithm), e.g. in [27, 40], the moduli space is given by $xy = zw^2$, with

$$x = X_{13}X_{32}X_{24}, \quad y = X_{31}X_{12}X_{23}, \quad z = X_{11}, \quad w = X_{13}X_{31} \tag{3.26}$$

modulo relations from the superpotential (namely, we also have e.g. $w = X_{12}X_{21}$). Using the mesons we have

$$x = X_{13}M_{31} \ , \ y = X_{31}M_{13} \ , \ z = X_{11} = M_{33} \ , \ w = X_{13}X_{31} = M_{11} \tag{3.27}$$

29

The monomials satisfy $xy - zw^2 = 0$ at the classical level, namely

$$X_{13}X_{31}(M_{31}M_{13} - M_{33}M_{11}) = 0 \qquad (3.28)$$

The quantum deformation of the moduli space of the field theory $M_{31}M_{13} - M_{33}M_{11} = \Lambda^4$, thus corresponds to

$$X_{13}X_{31}(M_{31}M_{13} - M_{33}M_{11}) = \epsilon X_{13}X_{31} \qquad (3.29)$$

which in terms of the monomials can be written as $xy - zw^2 = \epsilon w$ which is the description of the geometric deformation in Figure 15b. Thus the description we have provided has a quite direct link with the geometric description of the deformation, see Appendix B. Similar computations could be carried out in the other cases.

4. The dP_3 example

In this and subsequent sections we present examples where there are several scales of strong gauge dynamics along the RG flow. They are dual to supergravity solutions with several geometric features along the radial direction. The cleanest examples are those involving several deformation scales, which separate throat-like regions with different warp factors, dual to cascading flows in the gauge theory. In this section we center on one such example, based on the cone over dP_3.

The complex cone over dP_3 has two different deformation branches, shown in Figure 4. Following the discussion in section 2.4, it is possible to directly determine the sets of fractional branes in the gauge theory that are associated to the finite size 3-cycles in the supergravity description, and which should therefore trigger the corresponding RG flow and strong dynamics. In this section we carry out the gauge theory analysis corresponding to these sets of fractional branes and describe in detail the duality cascade and infrared dynamics.

Before doing that, let us review some general features of the gauge theory. The (p, q) web diagram is shown in Figure 4, and the corresponding quiver gauge theory is shown in figure 18. The superpotential reads (see e.g. [41])

$$W = X_{12}X_{23}X_{34}X_{45}X_{56}X_{61} + X_{13}X_{35}X_{51} + X_{24}X_{46}X_{62} -$$
$$- X_{23}X_{35}X_{56}X_{62} - X_{13}X_{34}X_{46}X_{61} - X_{12}X_{24}X_{45}X_{51} \qquad (4.1)$$

in self-explanatory notation.

A basis of fractional branes is given by the rank vectors $(1, 0, 0, 1, 0, 0)$, $(0, 0, 1, 0, 0, 1)$ and $(1, 0, 1, 0, 1, 0)$.
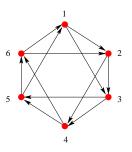
Figure 18: The quiver for D3-branes on the complex cone over dP_3.

4.1 The cascade for the first branch

In this section we describe a cascading RG flow for the dP_3 theory. This duality cascade, which has not appeared in the literature, provides the dual of the throat in [6] corresponding to the appropriate choice of fractional branes.

The cone over dP_3 has a two-dimensional deformation branch, shown in Figure 4c, which involves two independent 3-cycles and hence two independent RR fluxes. Hence a warped throat ending in this deformation must be dual to an RG flow in the quiver gauge theory with two independent fractional branes. From the geometry, and the argument in section 2.4, the 3-cycles involved in the deformation correspond to the fractional branes with rank vectors $(1, 0, 0, 1, 0, 0)$ and $(0, 0, 1, 0, 0, 1)$.

Hence our starting point is the quiver in Figure 18 with ranks

$$\vec{N} = N(1, 1, 1, 1, 1, 1) + P(1, 0, 0, 1, 0, 0) + M(0, 0, 1, 0, 0, 1) \tag{4.2}$$

In addition, the $\mathbb{Z}_2$ symmetry of the external legs in the toric diagram suggests that it is natural to consider initial conditions such that the RG flow is symmetric with respect to opposite nodes in the quiver. Hence, opposite nodes are taken with equal gauge couplings at a large UV scale. In order to study the RG flow to the infrared, we center on the regime $N \gg P \gg M$, which eventually will lead to two hierarchically different scales of RG flow.

The suggested duality cascade proceeds as follows. The nodes with largest beta function are 1 and 4, so we dualize them simultaneously. The results are shown in Figure 19a,b (the resulting quiver may be reordered to yield a standard maximally symmetric quiver, but we need not do so). Next the most strongly coupled nodes are 3, 6, so we dualize them simultaneously. This is shown in Figure 19b,c.

The quiver in Figure 19c can be reordered into a standard maximally symmetric quiver. This is of the form of the starting quiver, with similar fractional branes, but with the effective
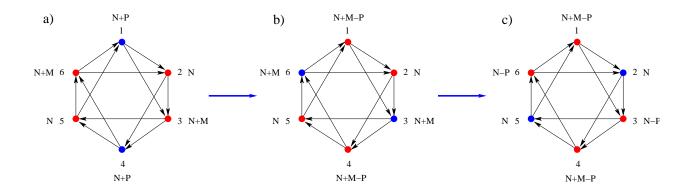
Figure 19: Two dualizations in the first RG cascade in dP_3. Dualized nodes are shown in blue.

N reduced by an amount P. We can then continue dualizing nodes 2, 5, then 1, 4, then 3, 6, etc, following the above pattern and generating a cascade which preserves the fractional branes but reduces the effective N.

In order to check that the suggested cascade of dualizations is consistent with an RG flow, we compute the gauge theories at each step in the cascade, along with the beta functions for the gauge couplings.

Given that $N \gg P \gg M$, we expect the cascade to be controlled by the P fractional branes of the first type in the UV. In that spirit, we study in detail the RG flow first neglecting the effect of M, which we set to zero for simplicity, under the assumption that the M fractional branes of the second type will only produce a small perturbation to the cascade constructed this way.

Let us explore in more detail that the above proposed cascade of dualizations 1,4,2,5,3,6 indeed corresponds to an RG flow. This cascade iterates between Models I and II of dP_3 in [42], and the corresponding ranks and beta functions at each step are

	N_1	N_2	N_3	N_4	N_5	N_6	β_1/P	β_2/P	β_3/P	β_4/P	β_5/P	β_6/P
1	$N+P$	N	N	$N+P$	N	N	**3**	$-3/2$	$-3/2$	3	$-3/2$	$-3/2$
2	$N-P$	N	N	$N+P$	N	N	-3	0	0	**3**	0	0
3	$N-P$	N	N	$N-P$	N	N	-3	**3/2**	$3/2$	-3	$3/2$	$3/2$
4	$N-P$	$N-P$	N	$N-P$	N	N	-2	$-3/2$	$5/2$	$-5/2$	**3/2**	2
5	$N-P$	$N-P$	N	$N-P$	$N-P$	N	$-3/2$	$-3/2$	**3**	$-3/2$	$-3/2$	3
6	$N-P$	$N-P$	$N-2P$	$N-P$	$N-P$	N	0	0	-3	0	0	**3**
7	$N-P$	$N-P$	$N-2P$	$N-P$	$N-P$	$N-2P$	$3/2$	$3/2$	-3	$3/2$	$3/2$	-3

$$(4.3)$$

After six dualizations (step **7** in the previous table), the quiver comes back to itself, with ranks

$$\vec{N} = (N - P)(1, 1, 1, 1, 1, 1) - P(0, 0, 1, 0, 0, 1) \tag{4.4}$$

Thus, the theory after six steps looks like the original one, with $N \to N - P$, plus a rotation and a replacement of $P \to -P$.

Notice that in the situation which is $\mathbb{Z}_2$ symmetric with respect to opposite nodes, the above duality steps group by pairs of simultaneous dualizations, and the quivers involved are always maximally symmetric (model I in [42]).

One may worry that in the presence of non-zero M the structure of the above cascade is destabilized. However, numerical results on the structure of cascades for a variety of choices of UV gauge couplings shows that the existence of cascades is a quite robust feature of the above choice of fractional branes (although the particular pattern of dualities involved in a cycle may be different from the above one).

Hence, the above cascade can be generalized to the situation with non-zero M, with the same result, namely there are cycles of Seiberg dualities, which leave the quiver and fractional branes invariant, but decrease the number of D3-branes in multiples of P.

The cascade proceeds until the effective N is not large compared with P. For simplicity, consider that the starting N is $N = (k+2)P - M$. Then after a suitable number of cascade steps, the ranks in the maximally symmetric quiver are $(2P-M, P-M, P, 2P-M, P-M, P)$, for nodes $(1, 2, 3, 4, 5, 6)$, as shown in Figure 20a. At this stage the $SU(2P - M)$ factors have $2P - M$ flavors and develop a quantum deformation of their moduli space. This should correspond to turning on one of the complex deformations of the geometry. From the structure of the left over web in the toric representation after a one-parameter deformation, see Figure 4b, we expect that the left over geometry should be a conifold. This is shown in Figure 20.

Before describing this quantum deformation in detail, let us simply mention that it results in the disappearance of nodes 1 and 4, the recombination of nodes 2 and 3, and 5 and 6 respectively, due to meson vevs, and a rearrangement of the arrows. The final result is indeed a conifold quiver gauge theory, with ranks $P - M$ and P. The theory subsequently evolves towards the infrared via a Klebanov-Strassler flow, by duality cascades where the effective number of D3-branes decreases in steps of M. At the end of this cascade, there is another condensation, which corresponds to turning on the second complex deformation of the cone over dP_3 to yield a smooth space.
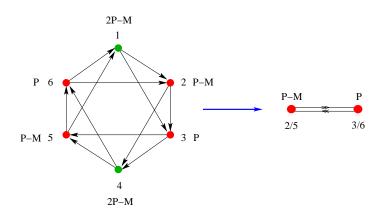
Figure 20: Condensation of the gauge theory of dP_3 to the gauge theory of the conifold. The nodes undergoing a deformation are indicated in green.
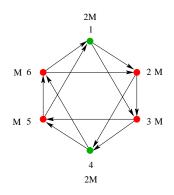

Figure 21: Gauge theory encoding the dynamics of D3-brane probes of the infrared of the cascade. The nodes undergoing a deformation are indicated in green.

4.2 The quantum deformation to the conifold

Let us now describe the fate of the dP_3 quiver theory at the end of the first duality cascade. To simplify the discussion, we take the situation where nodes 2356 have equal rank, i.e. $M = 0$, but the generalization to non-zero M is possible. We would like to consider the gauge theory associated to a set of P D3-branes probing the infrared of the duality cascade. The corresponding quiver is shown in Figure 21.

Following our general discussion in section 2.5, the $SU(2P)$ nodes condense, so we introduce the corresponding mesons

$$
\mathcal{M} = \begin{bmatrix} M_{63} & M_{62} \\ M_{53} & M_{52} \end{bmatrix} = \begin{bmatrix} X_{61}X_{13} & X_{61}X_{12} \\ X_{51}X_{13} & X_{51}X_{12} \end{bmatrix} \quad ; \quad \mathcal{N} = \begin{bmatrix} N_{36} & N_{35} \\ N_{26} & N_{25} \end{bmatrix} = \begin{bmatrix} X_{34}X_{46} & X_{34}X_{45} \\ X_{24}X_{46} & X_{24}X_{45} \end{bmatrix}
$$

We also introduce the baryons $\mathcal{B}$, $\tilde{\mathcal{B}}$, $\mathcal{A}$, $\tilde{\mathcal{A}}$. The quantum constraints read

$$\det \mathcal{M} - \mathcal{B}\tilde{\mathcal{B}} = \Lambda^{4P} \quad ; \quad \det \mathcal{N} - \mathcal{A}\tilde{\mathcal{A}} = \Lambda^{4P} \tag{4.5}$$

where we use the same dynamical scale for both gauge groups, corresponding to the $\mathbb{Z}_2$ symmetry of opposite nodes in the quiver preserved during the flow.

The superpotential reads

$$\begin{aligned} W = {} & M_{62}X_{23}N_{35}X_{56} + M_{53}X_{35} + N_{26}X_{62} - \\ & - X_{23}X_{35}X_{56}X_{62} - M_{63}N_{36} - M_{52}N_{25} + \\ & + X_1 \left(\det \mathcal{M} - \mathcal{B}\tilde{\mathcal{B}} - \Lambda^{4P} \right) + X_2 \left(\det \mathcal{N} - \mathcal{A}\tilde{\mathcal{A}} - \Lambda^{4P} \right) \end{aligned} \tag{4.6}$$

Going along the mesonic branch, we uncover the dynamics of the probes in the geometry at the infrared of the cascade. The mesonic branch corresponds to

$$X_1 = X_2 = \Lambda^{4-4P} \quad ; \quad \mathcal{A} = \tilde{\mathcal{A}} = 0 \quad ; \quad \mathcal{B} = \tilde{\mathcal{B}} = 0 \tag{4.7}$$

and the constraints on the mesons. For the most symmetric choice of meson vevs $\mathcal{M} \propto \mathbf{1}$, $\mathcal{N} \propto \mathbf{1}$, the gauge groups associated to the nodes 3 and 6, and 2 and 5, are broken to their respective diagonal combinations.

In order to simplify the discussion, we restrict to the Abelian case, where the superpotential reads

$$\begin{aligned} W = {} & M_{62}X_{23}N_{35}X_{56} - X_{23}X_{35}X_{56}X_{62} - M_{63}N_{36} - M_{52}N_{25} + \\ & + M_{53}X_{35} + N_{26}X_{62} + M_{63}M_{52} - M_{53}M_{62} + N_{36}N_{25} - N_{26}N_{35} \end{aligned} \tag{4.8}$$

Using the equations of motion for M_{53} and N_{26}, we have $X_{35} = M_{62}$, $X_{62} = N_{35}$. Thus

$$\begin{aligned} W = {} & X_{23}N_{35}X_{56}M_{62} - X_{23}M_{62}X_{56}N_{35} - \\ & - M_{63}N_{36} - M_{52}N_{25} + M_{63}M_{52} + N_{36}N_{25} \end{aligned} \tag{4.9}$$

Using the equations of motion for e.g. M_{63}, M_{52}, the quadratic terms disappear, and we are left with

$$W = X_{23}N_{35}X_{56}M_{62} - X_{23}M_{62}X_{56}N_{35} \tag{4.10}$$

Going back to the non-Abelian case, the gauge group is $SU(M)_{25} \times SU(M)_{36}$, with charged fields given by those appearing in the superpotential. These can be relabeled as $A_1 = X_{23}$

and $A_2 = X_{56}$, in the $(\square, \overline{\square})$, and $B_1 = M_{35}$, $B_2 = M_{62}$, in the $(\overline{\square}, \square)$. This is the gauge theory of D3-branes at a conifold singularity, showing that the left over geometry after the complex deformation is a conifold. It is important to note that there are some additional massless fields, which describe the dynamics of the D3-brane probe in the deformed geometry. Specifically, the quadratic terms in (4.9) leave two linear combinations of M_{63}, M_{52}, N_{36}, N_{25} massless. In addition, the fields M_{53} and N_{26}, which disappeared from the superpotential, also remain massless. Overall, we have light fields subject to the constraints (from $\partial W/\partial X_i = 0$)

$$M_{63}M_{52} - M_{53}M_{62} = \Lambda^{4P} \quad ; \quad N_{36}N_{25} - N_{26}N_{35} = \Lambda^{4P} \tag{4.11}$$

Hence the complete dynamics of the theory corresponds to one D3-probe in a geometry which is the deformation of a complex cone over dP_3 to a singular conifold.

Notice also that if we consider two kinds of fractional branes, namely non-zero M in the original cascade, the quantum deformation proceeds as above, since it involves recombinations of opposite nodes which have equal ranks even for non-zero M. The resulting condensation leads to a conifold, with the two nodes of the conifold theory having different ranks, what triggers a further Klebanov-Strassler duality cascade and infrared deformation.

4.3 The other branch

The cone over dP_3 has a second deformation branch, which is one-dimensional, see figure 4c. In this section we discuss the duality cascade dual to the corresponding supergravity throat, and describe the infrared deformation in the gauge theory.

Using the relation in section 2.4, the one-parameter deformation branch corresponds to the choice of fractional branes in Figure 22. Also, due to the $\mathbb{Z}_3$ symmetry of the geometry, it is natural to propose that nodes with even/odd label have equal UV couplings, respectively.

The proposed cascade in this case goes as follows. As one flows to the infrared, the $SU(N + M)$ gauge factors become strongly coupled and should be dualized. Their simultaneous dualization is difficult, since there are bi-fundamentals joining the corresponding nodes, so we proceed sequentially, with a particular choice of ordering which is not important for the final result. We choose to dualize node 1 first. The result is shown in Figure 23ab. In the resulting theory, there are no bi-fundamentals joining nodes 3 and 5, so we can now dualize them simultaneously, as shown in Figure 23bc.

Next, node 1 is most strongly coupled, so we dualize it again. The result is shown in Figure 24ab. Then, we dualize nodes 2 and 6. The final quiver is the maximally symmetric one, as can be shown by reordering the nodes as in 24bc. This final theory is of the same
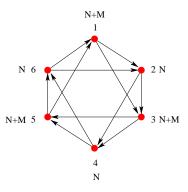
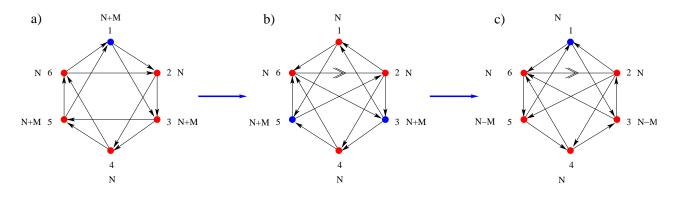**Figure 22:** Starting point of the cascade ending in the one-parameter deformation of the cone over dP_3.

Figure 23: Some steps in the duality cascade. Dualized nodes are shown in blue.

kind as the original one, but reducing the effective N in M units (and up to a rotation). Notice also that the final theory has the same nice $\mathbb{Z}_3$ symmetry between the nodes as the original onem with the nodes $(2, 4, 6)$ playing the role of $(1, 3, 5)$. One can then proceed to perform the same sequence of dualizations, this time on nodes $(2, 4, 6)$, completing a full cycle of the cascade.

The above heuristic derivation is confirmed by the detailed computation, and provides the field theory interpretation of the supergravity solution in [6], for the corresponding choice of asymptotic fluxes. The cascade proceeds until the effective number of D3-branes is comparable to that of fractional branes. At this stage, we may use the field theory to derive the strong infrared dynamics which removes the singularity by replacing it by a smooth deformed geometry.

For that purpose, we consider the dynamics of the theory at the end of the cascade, in the presence of additional D3-brane probes. Namely, we consider the quiver with ranks
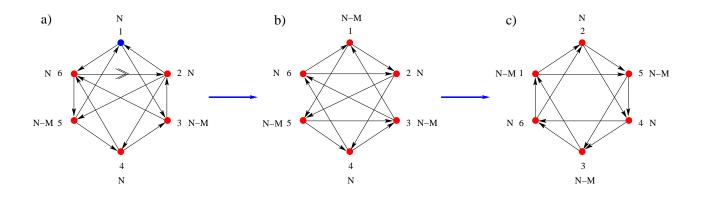
Figure 24: Last duality and reordering to complete the duality step. Note that the nodes of the last quiver have been reordered in order to make its $\mathbb{Z}_3$ symmetry manifest. The dualized node is shown in blue.

$(2M, M, 2M, M, 2M, M)$. In this situation, we expect that the three nodes 1, 3, 5 lead to a quantum deformed moduli space. In order to study the left-over theory, we consider performing this condensations sequentially (the order not being relevant for the final result).

Consider the strong dynamics associated to the node 1. We introduce the mesons

$$\mathcal{M} = \begin{bmatrix} M_{62} & M_{63} \\ M_{52} & M_{53} \end{bmatrix} = \begin{bmatrix} X_{61}X_{12} & X_{61}X_{13} \\ X_{51}X_{12} & X_{51}X_{13} \end{bmatrix} \tag{4.12}$$

Similar to our above analysis, we implement the quantum constraint in the superpotential. We center on the mesonic branch, along which the gauge factors 6 and 2, and 5 and 3, are broken to their respective diagonal subgroups, denoted 26 and 35 henceforth. Restricting to the Abelian case, the superpotential is described by

$$W = M_{62}X_{23}X_{34}X_{45}X_{56} + M_{53}X_{35} + X_{24}X_{46}X_{62} - X_{23}X_{35}X_{56}X_{62}$$
$$- M_{63}X_{34}X_{46} - M_{52}X_{24}X_{45} - M_{62}M_{53} + M_{52}M_{63} \tag{4.13}$$

The combined node 35 has $N_f = N_c$ plus additional massive adjoints and flavors, which we integrate out using the equations of motion for M_{53}, X_{35}, M_{52}, M_{63}. The resulting superpotential is

$$W = M_{62}X_{23}X_{34}X_{45}X_{56} + X_{24}X_{46}X_{62} - - X_{23}M_{62}X_{56}X_{62} - X_{34}X_{46}X_{24}X_{45} \tag{4.14}$$

so the only fields charged under the node 35 are the massless ones. Since it has $N_f = N_c$ we introduce the mesons

$$\mathcal{N} = \begin{bmatrix} N_{26} & N_{24} \\ N_{46} & N_{44} \end{bmatrix} = \begin{bmatrix} X_{23}X_{56} & X_{23}X_{34} \\ X_{45}X_{56} & X_{45}X_{34} \end{bmatrix} \tag{4.15}$$

which, along with the corresponding baryons, satisfy a quantum deformed constraint. Along the mesonic branch, the group associated to the nodes 26 and 4 is broken to a single diagonal combination. The superpotential is given by

$$W = M_{62}N_{24}N_{46} + X_{24}X_{46}X_{62} - N_{26}M_{62}X_{62} - N_{44}X_{46}X_{24} + N_{26}N_{44} - N_{46}N_{24} \quad (4.16)$$

Using the equations of motion for N_{26}, N_{44}, N_{46}, N_{24}, the superpotential reads

$$W = X_{24}X_{46}X_{62} - X_{24}X_{62}X_{46} \quad (4.17)$$

Since these fields transform in the adjoint representation of the leftover $SU(M)$ gauge group, this is the $\mathcal{N} = 4$ SYM theory, and the result implies that the geometry after the deformation is smooth. As usual, there are some additional neutral massless fields, with quantum modified constraints, which describe the dynamics of the probe in the deformation of dP_3 to a smooth geometry. We see that the complete smoothing by a single scale is in full agreement with the geometric picture.

5. Further examples

In this section we apply our by now familiar techniques to study other examples of quiver gauge theories with two scales of strong infrared dynamics.

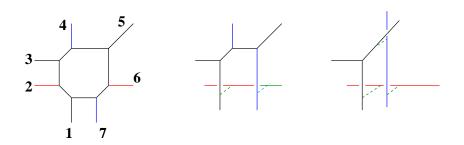### 5.1 From $PdP_4^{(I)}$ to the Suspended Pinch Point

We now investigate a two-scale cascade which follows the sequence

$$PdP_4^{(I)} \to SPP \to \text{smooth} \quad (5.1)$$

where PdP stands for 'pseudo del Pezzo' and $PdP_4^{(I)}$ indicates the complex cone over a non-generic toric blow-up of dP_3 denoted Model I of PdP_4 in [43].

This is another simple example of the agreement between the complex deformation of the geometry, and the quantum deformation of D3-branes probing the infrared theory of fractional branes. Since the discussion of the RG flow and existence of cascades in these geometries is involved and somewhat aside our main interest, we skip their discussion and center on the gauge theory description of the deformation.

We consider the theory on a stack of D3-branes probing a complex cone over the toric variety obtained by performing a non-generic blow-up of dP_3. Figure Figure 25a shows the (p, q) web diagram for this geometry. We also indicate a complex deformation to the suspended pinch point (SPP) singularity.

Figure 25: Web diagram for the $PdP_4^{(I)}$ model, its deformation to the SPP, and a further deformation to a smooth space.

The quiver diagram for this model is shown in Figure 26, which has a 5-block structure that is evident in the web diagram, with nodes 7, 1 and 2, 3 forming pairs.
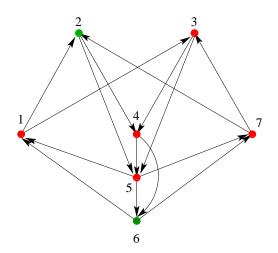

Figure 26: Quiver diagram for $PdP_4^{(I)}$. We show in green the nodes that undergo the deformation.

The corresponding superpotential was derived in [43] and reads

$$
\begin{aligned}
W = {} & X_{24}X_{46}X_{61}X_{12} + X_{73}X_{35}X_{57} - X_{73}X_{34}X_{46}X_{67} - X_{45}X_{57}X_{72}X_{24} \\
& - X_{35}X_{56}X_{61}X_{13} + X_{51}X_{13}X_{34}X_{45} - X_{25}X_{51}X_{12} + X_{25}X_{56}X_{67}X_{72}
\end{aligned}
\tag{5.2}
$$

Following our arguments in section 2.4, the deformation we want to consider corresponds, in the gauge theory, to the choice of fractional branes

$$
\vec{N} = M(1,1,1,1,1,1,1) + M(0,1,0,0,0,1,0)
\tag{5.3}
$$

Following our general prescription, we construct the meson fields for nodes 2 and 6

40

$$\mathcal{M} = \begin{bmatrix} M_{14} & M_{74} \\ M_{15} & M_{75} \end{bmatrix} = \begin{bmatrix} X_{12}X_{24} & X_{72}X_{24} \\ X_{12}X_{25} & X_{72}X_{25} \end{bmatrix}$$

(5.4)

$$\mathcal{N} = \begin{bmatrix} N_{41} & N_{47} \\ N_{51} & N_{57} \end{bmatrix} = \begin{bmatrix} X_{46}X_{61} & X_{46}X_{67} \\ X_{56}X_{61} & X_{56}X_{67} \end{bmatrix}$$

We now introduce Lagrange multiplier chiral fields to impose the quantum modified constraints on mesons and baryons. Along the mesonic branch we have

$$X_1 = \Lambda^{4-4M} \quad ; \quad \mathcal{B} = \tilde{\mathcal{B}} = 0 \quad ; \quad X_2 = \Lambda^{4-4M} \quad ; \quad \mathcal{C} = \tilde{\mathcal{C}} = 0$$

$$\det\mathcal{M} = \Lambda^{4M} \quad ; \quad \det\mathcal{N} = \Lambda^{4M} \tag{5.5}$$

Along the mesonic branch, nodes 1, 4 and 5, 7, recombine to their respective diagonal combinations. Restricting to the Abelian case, the superpotential is

$$\begin{aligned} W &= M_{14}N_{41} + X_{73}X_{35}X_{57} - X_{73}X_{34}N_{47} - X_{45}X_{57}M_{74} \\ &\quad -X_{35}N_{51}X_{13} + X_{51}X_{13}X_{34}X_{45} - M_{15}X_{51} + M_{75}N_{57} \\ &\quad -M_{14}M_{75} + M_{15}M_{74} - N_{41}N_{57} + N_{51}N_{47} \end{aligned} \tag{5.6}$$

Using the equations of motion for M_{14}, M_{15}, N_{57}, N_{47}, N_{51}, etc, we have

$$N_{41} = M_{75} \quad ; \quad X_{51} = M_{74} \quad ; \quad M_{75} = N_{41} \quad N_{51} = X_{73}X_{34} \quad ; \quad N_{47} = X_{35}X_{13} \tag{5.7}$$

The gauge group after symmetry breaking is $SU(N)_{57} \times SU(N)_{14} \times SU(N)_3$, and we have the superpotential

$$W = X_{73}X_{35}X_{57} - M_{74}X_{45}X_{57} - X_{73}X_{34}N_{47} - X_{35}X_{73}X_{34}X_{13} + M_{74}X_{13}X_{34}X_{45} \tag{5.8}$$

Relabeling the gauge group as $SU(N)_1 \times SU(N)_2 \times SU(N)_3$, and the fields as

$$M_{74} \to Y_{12} \quad , \quad X_{45} \to Y_{21} \quad , \quad X_{13} \to Y_{23} \quad , \quad X_{34} \to Y_{32}$$

$$X_{35} \to Y_{31} \quad , \quad X_{71} \to Y_{13} \quad , \quad X_{57} \to Y_{11} \tag{5.9}$$

we readily see the field content and superpotential of the SPP geometry. In addition to these fields, there are some massless modes, left over from the initial mesons. One can check that out of the eight original fields, five combinations remain massless, and they are subject to the quantum constraints, hence three degrees of freedom remain. They provide the moduli space of a D3-brane probe in the geometry given by the dP_4 deformed to a SPP.

The remaining theory may have fractional branes, triggering an RG flow related to the sequence of dualities discussed for SPP in section 3.3, which terminates in smooth $\mathbb{C}^3$.

5.2 From PdP_3b to $\mathbb{C}/\mathbb{Z}_2$

In this section we would like to discuss a further example of condensation, realized geometrically as the deformation of a non-generic blow-up of dP_2, the pseudo del Pezzo denoted PdP_3b in [36], to a $\mathbb{C}^2/\mathbb{Z}_2 \times \mathbb{C}$ orbifold singularity. From the geometric viewpoint, it illustrates the fact that different phases of the quiver gauge theory may suffer different condensation processes. From the field-theoretical viewpoint, it provides an example with a different behavior for the left over theory. Namely, instead of the $\mathcal{N} = 4$ theory or a conifold-like singularity, the left-over geometry corresponds to an orbifold singularity. In the presence of fractional branes on $\mathbb{C}^2/\mathbb{Z}_2$, the theory is not conformal, but instead of running down a cascade it encounters a singularity. The smoothing of this singularity in the dual supergravity description is of enhançon type [44].

Let us consider a set of branes at a complex cone over the non-generic blow-up of dP_2 leading to the quiver gauge theory in the phase denoted Model II of PdP_3b, worked out in [36], and whose quiver diagram is shown in Figure 27. The corresponding toric web diagram is shown in Figure 28 [11].
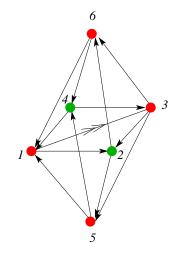

Figure 27: Quiver diagram for PdP_3b.

The tree level superpotential is given by

$$
\begin{aligned}
W_0 = {}& X_{12}X_{25}X_{54}X_{41} + X_{26}X_{64}X_{43}X_{32} - X_{25}X_{51}Y_{13}X_{32} - X_{64}X_{41}X_{13}X_{36} \\
& + Y_{13}X_{36}X_{61} + X_{13}X_{35}X_{51} - X_{61}X_{12}X_{26} - X_{43}X_{35}X_{54}
\end{aligned}
\tag{5.10}
$$

---

[11] Here we adhere to the terminology introduced in [36]. Thus, we see that the toric diagram for PdP_3b is different from the one for dP_3 and is given by the reciprocal of the (p, q) web in Figure 28.
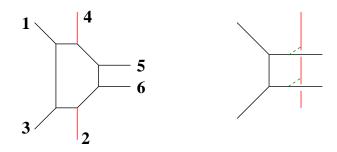
Figure 28: Web diagram for the cone over the non-generic blow-up of dP_2, and its deformation. The external legs have been labeled indicating their correspondence to the nodes in the quiver in Figure 27.

The geometric deformation of this space is shown in Figure 28b. Using our arguments in section 2.4, this corresponds to strong coupling dynamics associated to nodes 2 and 4 in the quiver diagram. In order to show this using D3-brane probes of this infrared dynamics, we consider the quiver gauge theory with rank vector

$$\vec{N} = M(0,1,0,1,0,0) + M(1,1,1,1,1,1) = M(1,2,1,2,1,1) \tag{5.11}$$

In this situation, the nodes 2 and 4 have $N_f = N_c$, and have a quantum deformed moduli space. Hence the above gauge theory (along the mesonic branch) describes the dynamics of D3-brane probes in the left over geometry after the complex structure deformation of the original geometry PdP_3. In the following, we follow the by now familiar arguments to determine the latter.

We introduce the meson fields

$$\mathcal{M} = \begin{bmatrix} M_{15} & M_{35} \\ M_{16} & M_{36} \end{bmatrix} = \begin{bmatrix} X_{12}X_{25} & X_{32}X_{25} \\ X_{12}X_{26} & X_{32}X_{26} \end{bmatrix}$$

$$\tag{5.12}$$

$$\mathcal{N} = \begin{bmatrix} N_{51} & N_{53} \\ N_{61} & N_{63} \end{bmatrix} = \begin{bmatrix} X_{54}X_{41} & X_{54}X_{43} \\ X_{64}X_{41} & X_{64}X_{43} \end{bmatrix}$$

In terms of mesons and baryons, the superpotential becomes

$$\begin{aligned} W = & M_{15}N_{51} + M_{36}N_{63} - M_{35}X_{51}Y_{13} - N_{61}X_{13}X_{36} \\ & + Y_{13}X_{36}X_{61} + X_{13}X_{35}X_{51} - M_{16}X_{61} - N_{53}X_{35} \\ & - X_1 \left(\det \mathcal{M} - \mathcal{B}\tilde{\mathcal{B}} - \Lambda^{4M} \right) - X_2 \left(\det \mathcal{N} - \mathcal{C}\tilde{\mathcal{C}} - \Lambda^{4M} \right) \end{aligned} \tag{5.13}$$

The mesonic branch is given by

$$X_1 = X_2 = \Lambda^{4-4M} \quad ; \quad \mathcal{B} = \tilde{\mathcal{B}} = 0 \quad ; \quad \mathcal{C} = \tilde{\mathcal{C}} = 0 \tag{5.14}$$

with the mesons subject to the quantum constraints. Also, along the mesonic branch, the symmetry is broken by recombining the gauge factors 1 and 5, and 3 and 6, into their respective diagonal combinations.

Restricting now to the Abelian case, the superpotential is

$$\begin{aligned}
W = {} & M_{15}N_{51} + M_{36}N_{63} - M_{35}X_{51}Y_{13} - N_{61}X_{13}X_{36} \\
& + Y_{13}X_{36}X_{61} + X_{13}X_{35}X_{51} - M_{16}X_{61} - N_{53}X_{35} \\
& - M_{15}M_{36} + M_{16}M_{35} - N_{51}N_{63} + N_{61}N_{53}
\end{aligned} \tag{5.15}$$

Using the equations of motion, we obtain e.g. $N_{61} = X_{35}$, $M_{16} = X_{61}$, $N_{51} = M_{36}$, $M_{15} = N_{63}$. The superpotential is

$$W = M_{35}X_{51}Y_{13} - N_{61}X_{13}X_{36} + Y_{13}X_{36}M_{16} + X_{13}N_{61}X_{51} \tag{5.16}$$

Relabeling the unbroken group as $SU(N)_A \times SU(N)_B$, and the fields as $Y_{13} \to X_{AB}$, $M_{35} \to X_{BA}$, $X_{51} \to \Phi_{AA}$, $X_{13} \to Y_{AB}$, $N_{61} \to Y_{BA}$, $X_{36} \to \Phi_{BB}$, the final quiver is presented in Figure 29.

Figure 29: Quiver diagram after deformation of PdP_3b. It corresponds to a $\mathbb{C}^2/\mathbb{Z}_2 \times \mathbb{C}$ geometry.

The field content and superpotential correspond to the gauge theory for a $\mathbb{C}^2/\mathbb{Z}_2 \times \mathbb{C}$ geometry. This agrees with the expected left over geometry after the complex deformation. In addition, the theory contains massless meson degrees of freedom, subject to the quantum constraint. They describe the dynamics of the D3-brane probe in the geometry given by the complex deformation of PdP_3 to $\mathbb{C}^2/\mathbb{Z}_2 \times \mathbb{C}$.

As usual, it is possible to study the situation where the final gauge theory contains fractional branes. This theory is $\mathcal{N} = 2$ supersymmetric, hence its RG evolution could be determined from its exact solution. As usual in non-conformal $\mathcal{N} = 2$ theories, instead of a duality cascade we expect strong coupling singularities. In the dual supergravity side, they are described as enhançon configurations [44].

6. Conclusions

In this paper we have centered on the gauge field theory dynamics associated to the smoothing of singularities in warped throat solutions dual to RG flows for branes at singularities in the presence of fractional branes. We have established that in a large set of examples the

smoothing corresponds to a complex deformation of the cone geometries. We have described this phenomenon in the dual gauge field theory, by using D3-brane probes of the infrared dynamics. The geometric deformation arises as a quantum deformation of the moduli space of the D3-brane probes. The field theory description is in full agreement with the geometric description of the complex deformation using toric methods.

In addition, we have constructed new explicit examples of cascading RG flows for some of these theories. These duality cascades, along with the infrared deformations, are generalizations of the Klebanov-Strassler RG flow, but show a richer structure in several respects. For instance, very interestingly, several examples correspond to duality cascades with several scales of partial confinement and deformation, after each of which the remaining quiver theory continues cascading down the infrared in a different pattern. Their supergravity duals should correspond to warped throats whose warp factor and flux structure jumps at particular values of the radial coordinate. In other words, to warped throats based on a deformed geometry with several 3-cycles, which are of hierarchically different size. It would be interesting to develop a better understanding of these throats directly from the supergravity side. Also, we expect several interesting applications of these richer throat structures to compactification and model building [32].

Our work opens a set of new questions. For instance, certain geometries do admit fractional branes, and even have known KT-like warped throat solutions, but do not admit complex deformations to smooth out their singularities. It would be interesting to understand the infrared behavior of this class of models. In particular, the real cones over the recently studied $Y^{p,q}$ manifolds, of which the five-dimensional horizon of the complex cone over dP_1 is an example, fall in this class. We hope interesting progress in this direction.

Finally, there is an interesting phenomenon taking place in the quiver gauge theories we have studied, which is however not involved in the nice RG flows we have centered on. Namely, some of these theories, for other choices of fractional branes (or of UV gauge couplings) exhibit duality walls [3, 4, 45, 6]. It is conceivable that a gauge theory with in principle a duality wall in its UV can actually be UV completed by regarding it as a remnant after confinement of a larger gauge theory at higher energies, with a better behaved UV regime. Thus our work may shed some light also into these more exotic RG flows. We leave this and other questions for future research.

Acknowledgements

A. A more careful look at the mesonic branch

In this appendix we present an alternative approach to the field theory analysis of the IR complex deformation of the geometry, which complements our methods in Section 2.5. The strategy will be to consider the dynamics of the fluctuations of the meson fields around the expectation values required by the quantum constraints. As we will see, this method has the advantage of clarifying how the relative signs of the Lagrange multipliers are determined and shows how the low energy limit with respect to the strong coupling scales is taken explicitly.

In order to illustrate these ideas, we will focus in the example of the deformation from dP_3 down to the conifold. We will reproduce the computations performed in Section 4.2 from a different viewpoint.

As discussed, the quantum modified constraints on the meson and baryon fields (2.21) are imposed via Lagrange multipliers X_i. The quiver for the phase of dP_3 we are considering is shown in Figure 21. The ranks are

$$\vec{N} = M(1,1,1,1,1,1) + M(1,0,0,1,0,0) \tag{A.1}$$

leading to a quantum modified moduli space for nodes 1 and 4. The meson fields for these nodes are

$$\mathcal{M} = \begin{bmatrix} M_{63} & M_{62} \\ M_{53} & M_{52} \end{bmatrix} = \begin{bmatrix} X_{61}X_{13} & X_{61}X_{12} \\ X_{51}X_{13} & X_{51}X_{12} \end{bmatrix} \quad ; \quad \mathcal{N} = \begin{bmatrix} N_{36} & N_{35} \\ N_{26} & N_{25} \end{bmatrix} = \begin{bmatrix} X_{34}X_{46} & X_{34}X_{45} \\ X_{24}X_{46} & X_{24}X_{45} \end{bmatrix}$$

In terms of them and the baryonic operators, the quantum corrected superpotential is

$$W = M_{62}X_{23}N_{35}X_{56} - X_{23}X_{35}X_{56}X_{62} - M_{63}N_{36} - M_{52}N_{25} + M_{53}X_{35} + N_{26}X_{62}$$

$$+ X_1(\det M - B\tilde{B} - \Lambda^{4M}) + X_2(\det N - C\tilde{C} - \Lambda^{4M}) \tag{A.2}$$

Let us focus on the mesonic branch of the moduli space, i.e. solutions with $\mathcal{B} = \tilde{\mathcal{B}} = \mathcal{C} = \tilde{\mathcal{C}} = 0$.

$$\begin{aligned} \partial_{X_1} W = 0 &\Rightarrow \det \mathcal{M} = \Lambda^{4M} \\ \partial_{X_2} W = 0 &\Rightarrow \det \mathcal{N} = \Lambda^{4M} \end{aligned} \tag{A.3}$$

For simplicity, we concentrate on a particularly simple choice of vev's satisfying (A.3)

$$< \mathcal{M} >= \Lambda^2 \begin{bmatrix} 1_{M \times M} & 0 \\ 0 & 1_{M \times M} \end{bmatrix} \qquad < \mathcal{N} >= \Lambda^2 \begin{bmatrix} 1_{M \times M} & 0 \\ 0 & 1_{M \times M} \end{bmatrix} \tag{A.4}$$

Denoting η_{ij} and ξ_{ij} the fluctuations of M_{ij} and N_{ij} around their respective expectation values, and dropping a constant term, the superpotential in the Abelian case becomes

$$\begin{aligned} W = {}& \eta_{62} X_{23} \eta_{35} X_{56} - X_{23} X_{35} X_{56} X_{62} - 2\Lambda^4 - \Lambda^2(\eta_{63} + \eta_{36} + \eta_{52} + \eta_{25}) \\ &- \eta_{63}\eta_{36} - \eta_{52}\eta_{25} + \eta_{53} X_{35} + \eta_{26} X_{62} \\ &+ X_1(\Lambda^2(\eta_{63} + \eta_{52}) + \eta_{63}\eta_{52} - \eta_{53}\eta_{62}) + X_2(\Lambda^2(\eta_{36} + \eta_{25}) + \eta_{36}\eta_{25} - \eta_{35}\eta_{26}) \end{aligned} \tag{A.5}$$

We are interested in looking at energies much smaller than the dynamical scale Λ. This can be systematically implemented by taking the large Λ limit of the superpotential, which we will call W', and looking at the approximate equations of motion that follow. For large Λ, the superpotential becomes

$$W' = -\Lambda^2(\eta_{63} + \eta_{52}) - \Lambda^2(\eta_{36} + \eta_{25}) - \Lambda^2 X_1(\eta_{63} + \eta_{52}) - \Lambda^2 X_2(\eta_{36} + \eta_{25}) + \mathcal{O}(\Lambda^0) \tag{A.6}$$

This determines the value of the Lagrange multipliers through

$$\begin{aligned} \frac{\partial W'}{\partial(\eta_{63} + \eta_{52})} = 0 &\rightarrow X_1 = 1 \\ \frac{\partial W'}{\partial(\eta_{36} + \eta_{25})} = 0 &\rightarrow X_2 = 1 \end{aligned} \tag{A.7}$$

Plugging this into (A.5), we obtain an expression identical to (4.8), with the mesons replaced by their corresponding fluctuations. The rest of the proof is the same as the one in Section 4.2.

This type of discussion makes clear, for example, how the relative minus sign in the values of the Lagrange multipliers X_1 and X_2 assumed in (3.13) is determined.

47

B. Description of complex deformations

In this section we provide a precise geometric description of the complex deformation corresponding to the removal of sub-webs in the toric diagram of our geometries. For additional details and other examples see [46].

The basic process in the separation of a sub-web in a toric diagram is the separation of two lines. This basic process is already present in the complex deformation of the conifold. In order to describe it in toric language, recall the toric data for the conifold

$$\begin{array}{ccccc} & a_1 & a_2 & b_1 & b_2 \\ Q & 1 & 1 & -1 & -1 \end{array}$$

Namely, one is performing a Kahler quotient of $\mathbb{C}^4$ by the $U(1)$ action acting on it with the above charges. Physically, the conifold is the target of the 2d linear sigma model specified by the above charges for a set of four chiral multiplets. The moment map equation (equivalently the D-term equations for the linear sigma model) are

$$|a_1|^2 + |a_2|^2 - |b_1|^2 - |b_2|^2 = s \tag{B.1}$$

The geometry is toric, namely can be regarded as a fibration of circles over a base. The $U(1)$ action is simply generated by the three independent phase rotations of the chiral multiplets, up to the above $U(1)$ action (which is a gauge equivalence).

The geometry can be describe using the gauge-invariant quantities $x = a_1a_2$, $y = b_1b_2$, $u = a_1b_1$, $v = a_2b_2$, as the hypersurface in $\mathbb{C}^4$ defined by $xy = uv$. This may be equivalently described by the two equations $xy = z$, $uv = z$. The $U(1)$ actions degenerate along lines in the subspace $z = 0$. The toric projection in Figure 30 describes the loci in $z = 0$ where the $U(1)$ actions degenerate. Notice that s measures the size of the 2-cycle in the resolved conifold.
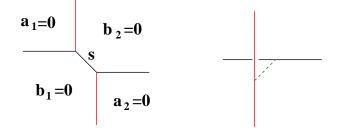

Figure 30: Toric projection and complex deformation for the conifold.

The complex deformation involving the separation of the two lines, Figure 30b, is possible when $s = 0$. To describe it, we simply use monomials invariant under the $U(1)$ gauge

symmetry associated to s, namely x, y, u, v, and deform their constraint to

$$xy - uv = \epsilon \tag{B.2}$$

This may be recast as $xy = z + \epsilon$, $uv = z$, showing that there are two different values of z at which the toric fibers degenerate. This implies that the two lines have separated from each other.
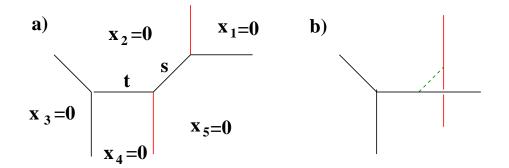

Figure 31: Toric projection and complex deformation for the SPP.

The procedure generalizes to more involved situations. Let us consider the SPP singularity, for which the toric data are

$$
\begin{array}{c c c c c c}
 & x_1 & x_2 & x_3 & x_4 & x_5 \\
Q_s & 1 & -1 & 0 & 1 & -1 \\
Q_t & 0 & 0 & 1 & -2 & 1
\end{array}
$$

The corresponding D-term equations are

$$|x_1|^2 + |x_4|^2 - |x_2|^2 - |x_5|^2 = s,$$
$$|x_3|^2 + |x_5|^2 - 2|x_4|^2 = t \tag{B.3}$$

There are two parameters s, t which control the size of two independent 2-cycles in the geometry. The toric picture, showing the degeneration loci of the toric circle actions, is shown in Figure 31a. The complex structure of the SPP is given by

$$uv = xy^2, \tag{B.4}$$

where x, y, u, v are gauge invariant coordinates,

$$x = x_1 x_2, \quad y = x_3 x_4 x_5, \quad u = x_1 x_4 x_5^2, \quad v = x_2 x_3^2 x_4. \tag{B.5}$$

The complex structure deformation, in Figure 31b, arises when $s = 0$. In order to describe it, we introduce variables invariant under $U(1)_s$

$$x = x_1 x_2, \quad y = x_3 x_4 x_5 \quad \rho = x_1 x_5 / x_3 \quad v = x_2 x_3^2 x_4 \qquad (B.6)$$

(which are well-defined for $x_3 \neq 0$). They satisfy a constraint $x\tilde{y} = \rho\tilde{v}$, which we deform to

$$xy - \rho v = \epsilon \qquad (B.7)$$

In the complete manifold, using that $\rho = u/y$, we obtain for the complex deformation

$$xy^2 = (\rho v + \epsilon) y = uv + \epsilon y \qquad (B.8)$$

Notice that this geometric argument and the deformed geometry nicely dovetail the field theory argument at the end of section 3.3.

C. Cones over the $Y^{p,q}$ manifolds

Real cones over the manifolds $Y^{p,q}$ [7, 8, 9, 10, 11] provide an infinite family of 6 dimensional singular geometries on which we can place D3-branes. This leads to an infinite class of quiver gauge theories, which have been determined in [12], and whose study is a promising new direction in the gauge/gravity correspondence.

One interesting feature is that the five dimensional $Y^{p,q}$ manifolds have only one collapsing 2-cycle and thus admit a single kind of fractional brane, which triggers a cascading RG flow. Some particular cascades, as well as the KT-like supergravity solutions for the general case, have been recently constructed in [13]. The warped throat solutions contain a naked singularity at their tip. A natural question is whether a smooth solution exists, based on a complex deformation of the underlying geometry, and how to understand it from the dual field theory viewpoint.

In general these 6 dimensional manifolds correspond to spaces which do not admit complex deformations. This can be seen from the web diagrams of those spaces, see Figure 32.

Only in the case of $Y^{p,0}$ a decomposition of the web into sub-webs is possible. This case is also special, since it corresponds to a $\mathbb{Z}_p$ quotient of the conifold. More concretely, defining the conifold by the equation
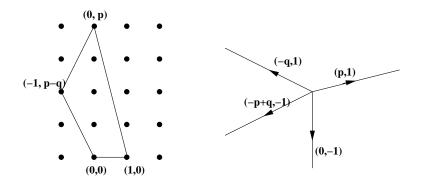
$$xy - zw = 0 \qquad (C.1)$$

Figure 32: The toric and web diagram for the cone over the general $Y^{p,q}$ manifold. No leg recombination is possible except for the case $q = 0$.

the cone over $Y^{p,0}$ is obtained by modding out by the $\mathbb{Z}_p$ action generated by θ, which acts as

$$x \to e^{2\pi i/p} x \quad , \quad y \to e^{-2\pi i/p} y \quad , \quad z \to e^{2\pi i/p} z \quad , \quad w \to e^{-2\pi i/p} w \tag{C.2}$$

which is clearly a symmetry of (C.1).

The complex deformation of the manifold is simply the $\mathbb{Z}_p$ quotient of the complex deformation of the conifold

$$xy - zw = \epsilon \tag{C.3}$$

The 3-cycle in the deformed space is the Lens space $S^3/\mathbb{Z}_p$.

Therefore, although both warped supergravity throats and logarithmic RG duality cascades seem to exist for all the $Y^{p,q}$ cases, the class of $Y^{p,0}$ manifolds stand out as the only cases which admit a complex deformation, presumably removing the infrared singularity of their supergravity solutions. Our plan is to center on this class and indeed derive the deformation from the viewpoint of the strong dynamics of the dual gauge theory with fractional branes in general.

For that purpose we need the corresponding quiver gauge theories. These can be obtained using the rules in [12], but for illustration purposes we construct them using their realization as $\mathbb{Z}_p$ quotients of the conifold. This can be done following the ideas in [39]. Concretely, the conifold theory is $SU(N_1) \times SU(N_2)$ with fields A_1, A_2 in the $(\square, \overline{\square})$ and B_1, B_2 in the $(\overline{\square}, \square)$. We also have the superpotential

$$W = A_1 B_1 A_2 B_2 - A_1 B_2 A_2 B_1 \tag{C.4}$$

By the realization of the conifold as the moduli space of the gauge theory, there is a relation between the fields and the coordinates x, y, z, w. Roughly

$$x \simeq A_1 B_1 \quad , \quad y \simeq A_2 B_2 \quad , \quad z \simeq A_1 B_2 \quad , \quad w \simeq A_2 B_1 \qquad \text{(C.5)}$$

The action (C.2) can thus be implemented as the action

$$A_1 \to e^{2\pi i/p} A_1 \quad , \quad A_2 \to e^{-2\pi i/p} A_2 \quad , \quad B_1 \to B_1 \quad , \quad B_2 \to B_2 \qquad \text{(C.6)}$$

In addition, we have to specify the action of θ on the $SU(N_1)$ and $SU(N_2)$ Chan-Paton labels. This is done by two order p discrete gauge transformations, which without loss of generality can be chosen

$$\gamma_{\theta,1} = \text{diag}\left(\mathbf{1}_{n_0}, e^{2\pi i/p}\mathbf{1}_{n_1}, \ldots, e^{2\pi i(p-1)/p}\mathbf{1}_{n_{p-1}}\right)$$
$$\gamma_{\theta,2} = \text{diag}\left(\mathbf{1}_{m_0}, e^{2\pi i/p}\mathbf{1}_{m_1}, \ldots, e^{2\pi i(p-1)/p}\mathbf{1}_{m_{p-1}}\right) \qquad \text{(C.7)}$$

with $\sum_a n_a = N_1$ and $\sum_a m_a = N_2$.

Now we have to project with respect to the combined geometric and Chan-Paton action. For vector multiplets, the geometric action is trivial, and we simply get a gauge group

$$SU(n_0) \times \ldots \times SU(n_{p-1}) \times SU(m_0) \times \ldots \times SU(m_{p-1}) \qquad \text{(C.8)}$$

while the projection for the chiral multiplets leads to a set of chiral multiplets in the following representations

$$(A_1)_{a,a+1} = (n_a, \overline{m}_{a+1}) \qquad (A_2)_{a,a-1} = (n_a, \overline{m}_{a-1})$$
$$(B_1)_{a,a} \;\;= (\overline{n}_a, m_a) \qquad (B_2)_{a,a} \;\;= (\overline{n}_a, m_a) \qquad \text{(C.9)}$$

The superpotential is directly obtained from the conifold one and reads

$$W = \sum_a \left[(A_1)_{a,a+1}(B_1)_{a+1,a+1}(A_2)_{a+1,a}(B_2)_{a,a} - (A_1)_{a,a+1}(B_2)_{a+a,a+1}(A_2)_{a+1,a}(B_1)_{a,a}\right]$$

The complete result agrees with that using the rules in [12] (by relabeling $B_\alpha \to U^\alpha$, $A_1 \to Z$, $A_2 \to Y$). It is easy to check that the quiver for e.g. $Y_{4,0}$ agrees with that in figure 8 in [12].

This gauge theory admits a single kind of fractional brane. The gauge theory corresponds to $n_a = N + M$, and $m_a = N$. The RG flow presumably leads to a cascade of Seiberg dualities with structure very similar to that of the conifold. Although we have not carried

out a complete analysis, we would like to make the following natural proposal. Consider all the nodes $SU(N)$ to have equal coupling at some UV scale, and all nodes $SU(N + M)$ to have equal coupling. Namely, we consider the couplings to respect the $\mathbb{Z}_p$ symmetry of the quiver. As we run to the IR, the nodes $SU(N + M)$ get to strong coupling. Let us Seiberg dualize them simultaneously (to do it in practice, we may do it sequentially, but presumably the order is not important). After this, we obtain a similar quiver, with all ranks $N + M$ replaced by $N - M$. So next one should dualize all the nodes of rank N, etc. This just amounts to inheriting the cascade from the parent to the orbifold theory.

Let us now consider the infrared behavior of the cascade. For N a multiple of M (in which case we center in what follows) the endpoint of the cascade is a theory of p decoupled $N = 1$ SYM nodes, with equal gauge coupling (or dynamical scale) due to the $\mathbb{Z}_p$ symmetry of the flow. The unique dynamical scale should be associated with a finite-size 3-cycle in a deformed geometry.

In order to check that the geometry at the tip of the throat is the deformed geometry described above, we consider the gauge theory describing the dynamics of M D3-brane probing the IR theory. Namely, using the by now familiar technique we take the quiver theory with group

$$\prod_a SU(2M)_a \times \prod_a SU(M)_a \tag{C.10}$$

The nodes $SU(2M)_a$ condense, so we introduce the mesons

$$\mathcal{M} = \begin{bmatrix} M_{a,a+1} \ \tilde{M}_{a,a+1} \\ M_{a,a-1} \ \tilde{M}_{a,a-1} \end{bmatrix} = \begin{bmatrix} (A_1)_{a,a+1}(B_1)_{a+1,a+1} \ (A_1)_{a,a+1}(B_2)_{a+1,a+1} \\ (A_2)_{a,a-1}(B_1)_{a-1,a-1} \ (A_2)_{a,a-1}(B_2)_{a-1,a-1} \end{bmatrix} \tag{C.11}$$

In terms of these, the superpotential reads

$$W = \sum_a \left[M_{a,a+1}\tilde{M}_{a+1,a} - \tilde{M}_{a,a+1}M_{a+1,a} \right] \tag{C.12}$$

We now should impose the quantum constraint, and pick the mesonic branch. Along the mesonic branch, all the $SU(M)_a$ gauge groups are broken to a single diagonal combination. Therefore all mesons transform in the adjoint representation of this gauge group. Imposing the constraint as a superpotential and centering in the Abelian case as usual, we have

$$W = \sum_a \left[M_{a,a+1}\tilde{M}_{a+1,a} - \tilde{M}_{a,a+1}M_{a+1,a} - M_{a,a+1}\tilde{M}_{a,a-1} + M_{a,a-1}\tilde{M}_{a,a+1} \right] \tag{C.13}$$

Notice that we have $4pM^2$ meson degrees of freedom. However, they have to satisfy the F-term equations

$$\tilde{M}_{a+1,a} = \tilde{M}_{a,a-1} \qquad M_{a+1,a} = M_{a,a-1}$$

$$\tilde{M}_{a,a+1} = \tilde{M}_{a-1,a} \qquad M_{a,a+1} = M_{a-1,a} \tag{C.14}$$

These are apparently $4pM^2$ relations. However, they are not all independent. This can be seen by noticing that they only fix the relative vevs of the mesons for different values of a, but they do not fix the overall size of a given kind of meson. Therefore, there are four operators whose vevs are not fixed by the above conditions. They are

$$M_{11} = \prod_a M_{a,a+1} \quad , \quad M_{12} = \prod_a \tilde{M}_{a,a+1} \quad , \quad M_{21} = \prod_a M_{a+1,a} \quad , \quad M_{22} = \prod_a \tilde{M}_{a+1,a} \tag{C.15}$$

Notice however that the original mesons are also constrained by the quantum constraint (which is obtained from $\partial W / \partial X_a = 0$ before going into the mesonic branch etc). This implies that the final operators have to satisfy

$$M_{11}M_{22} - M_{12}M_{21} = \Lambda^P \tag{C.16}$$

This moduli space indeed corresponds to a deformed space. Moreover, the fact that the fundamental mesons are related to the above fields by the order p relation (C.15) shows that the final space is a $\mathbb{Z}_p$ quotient of the deformed conifold.

Hence the whole family of $Y^{p,0}$ cones is closely related to the KS conifold, and a generalization of the complex cone over F_0, which is the case $p = 2$ in the above language. The field theory argument plus the geometric analysis strongly support the existence of a smooth supergravity solution describing a complete RG flow for these theories. Indeed, these exist and are given simply by the $\mathbb{Z}_p$ quotient of the KS solution.

References

[1] I. R. Klebanov and E. Witten, "Superconformal field theory on threebranes at a Calabi-Yau singularity," Nucl. Phys. B **536**, 199 (1998) [arXiv:hep-th/9807080].

[2] I. R. Klebanov and M. J. Strassler, "Supergravity and a confining gauge theory: Duality cascades and χSB-resolution of naked singularities," JHEP **0008**, 052 (2000) [arXiv:hep-th/0007191].

[3] A. Hanany and J. Walcher, "On duality walls in string theory," JHEP **0306**, 055 (2003) [arXiv:hep-th/0301231].

[4] S. Franco, A. Hanany, Y. H. He and P. Kazakopoulos, "Duality walls, duality trees and fractional branes," arXiv:hep-th/0306092.

[5] I. R. Klebanov and A. A. Tseytlin, "Gravity duals of supersymmetric SU(N) x SU(N+M) gauge theories," Nucl. Phys. B **578**, 123 (2000) [arXiv:hep-th/0002159].

[6] S. Franco, Y. H. He, C. Herzog and J. Walcher, "Chaotic duality in string theory," Phys. Rev. D **70**, 046006 (2004) [arXiv:hep-th/0402120].

[7] J. P. Gauntlett, D. Martelli, J. Sparks and D. Waldram, "Supersymmetric AdS(5) solutions of M-theory," Class. Quant. Grav. **21**, 4335 (2004) [arXiv:hep-th/0402153].

[8] J. P. Gauntlett, D. Martelli, J. Sparks and D. Waldram, "Sasaki-Einstein metrics on S^2 x S^3," arXiv:hep-th/0403002.

[9] J. P. Gauntlett, D. Martelli, J. F. Sparks and D. Waldram, "A new infinite class of Sasaki-Einstein manifolds," arXiv:hep-th/0403038.

[10] J. P. Gauntlett, D. Martelli, J. Sparks and D. Waldram, "Supersymmetric AdS backgrounds in string and M-theory," arXiv:hep-th/0411194.

[11] D. Martelli and J. Sparks, "Toric geometry, Sasaki-Einstein manifolds and a new infinite class of AdS/CFT duals," arXiv:hep-th/0411238.

[12] S. Benvenuti, S. Franco, A. Hanany, D. Martelli and J. Sparks, "An infinite family of superconformal quiver gauge theories with Sasaki-Einstein duals," arXiv:hep-th/0411264.

[13] Q. J. Ejaz, C. P. Herzog and I. R. Klebanov, "Cascading RG Flows from New Sasaki-Einstein Manifolds," arXiv:hep-th/0412193.

[14] M. Bertolini, F. Bigazzi and A. L. Cotrone, "New checks and subtleties for AdS/CFT and a-maximization," JHEP **0412**, 024 (2004) [arXiv:hep-th/0411249].

[15] S. S. Gubser, "Supersymmetry and F-theory realization of the deformed conifold with three-form flux," arXiv:hep-th/0010010.

[16] M. Graña and J. Polchinski, "Supersymmetric three-form flux perturbations on AdS(5)," Phys. Rev. D **63**, 026001 (2001) [arXiv:hep-th/0009211].

[17] C. Vafa, "Superstrings and topological strings at large N," J. Math. Phys. **42**, 2798 (2001) [arXiv:hep-th/0008142].

[18] F. Cachazo, K. A. Intriligator and C. Vafa, "A large N duality via a geometric transition," Nucl. Phys. B **603**, 3 (2001) [arXiv:hep-th/0103067].

[19] F. Cachazo, S. Katz and C. Vafa, "Geometric transitions and N = 1 quiver theories," arXiv:hep-th/0108120.

[20] F. Cachazo, B. Fiol, K. A. Intriligator, S. Katz and C. Vafa, "A geometric unification of dualities," Nucl. Phys. B **628**, 3 (2002) [arXiv:hep-th/0110028].

[21] O. Aharony and A. Hanany, "Branes, superpotentials and superconformal fixed points," Nucl. Phys. B **504**, 239 (1997) [arXiv:hep-th/9704170].

[22] O. Aharony, A. Hanany and B. Kol, "Webs of (p,q) 5-branes, five dimensional field theories and grid diagrams," JHEP **9801**, 002 (1998) [arXiv:hep-th/9710116].

[23] N. C. Leung and C. Vafa, "Branes and toric geometry," Adv. Theor. Math. Phys. **2**, 91 (1998) [arXiv:hep-th/9711013].

[24] S. S. Gubser, C. P. Herzog and I. R. Klebanov, "Symmetry breaking and axionic strings in the warped deformed conifold," JHEP **0409**, 036 (2004) [arXiv:hep-th/0405282].

[25] M. Schvellinger, "Glueballs, symmetry breaking and axionic strings in non-supersymmetric deformations of the Klebanov-Strassler background," JHEP **0409**, 057 (2004) [arXiv:hep-th/0407152].

[26] A. Butti, M. Graña, R. Minasian, M. Petrini and A. Zaffaroni, "The baryonic branch of Klebanov-Strassler solution: A supersymmetric family of SU(3) structure backgrounds," arXiv:hep-th/0412187.

[27] D. R. Morrison and M. R. Plesser, "Non-spherical horizons. I," Adv. Theor. Math. Phys. **3**, 1 (1999) [arXiv:hep-th/9810201].

[28] K. Dasgupta, G. Rajesh and S. Sethi, "M theory, orientifolds and G-flux," JHEP **9908**, 023 (1999) [arXiv:hep-th/9908088].

[29] S. B. Giddings, S. Kachru and J. Polchinski, "Hierarchies from fluxes in string compactifications," Phys. Rev. D **66**, 106006 (2002) [arXiv:hep-th/0105097].

[30] S. Kachru, R. Kallosh, A. Linde, J. Maldacena, L. McAllister and S. P. Trivedi, "Towards inflation in string theory," JCAP **0310**, 013 (2003) [arXiv:hep-th/0308055].

[31] J. F. G. Cascales, M. P. Garcia del Moral, F. Quevedo and A. M. Uranga, "Realistic D-brane models on warped throats: Fluxes, hierarchies and moduli stabilization," JHEP **0402**, 031 (2004) [arXiv:hep-th/0312051].

[32] J. F. G. Cascales, F. Saad, A. M. Uranga, to appear.

[33] F. Denef and M. R. Douglas, "Distributions of flux vacua," JHEP **0405**, 072 (2004) [arXiv:hep-th/0404116].

[34] N. Seiberg, "Five dimensional SUSY field theories, non-trivial fixed points and string dynamics," Phys. Lett. B **388**, 753 (1996) [arXiv:hep-th/9608111].

[35] D. R. Morrison and N. Seiberg, "Extremal transitions and five-dimensional supersymmetric field theories," Nucl. Phys. B **483**, 229 (1997) [arXiv:hep-th/9609070].

[36] B. Feng, Y. H. He and F. Lam, "On correspondences between toric singularities and (p,q)-webs," arXiv:hep-th/0403133.

[37] A. Hanany and A. Iqbal, "Quiver theories from D6-branes via mirror symmetry," JHEP **0204**, 009 (2002) [arXiv:hep-th/0108137].

[38] S. Franco and A. Hanany, "Geometric dualities in 4d field theories and their 5d interpretation," JHEP **0304**, 043 (2003) [arXiv:hep-th/0207006].

[39] A. M. Uranga, "Brane configurations for branes at conifolds," JHEP **9901**, 022 (1999) [arXiv:hep-th/9811004].

[40] J. Park, R. Rabadan and A. M. Uranga, "Orientifolding the conifold," Nucl. Phys. B **570**, 38 (2000) [arXiv:hep-th/9907086].

[41] B. Feng, S. Franco, A. Hanany and Y. H. He, "Symmetries of toric duality," JHEP **0212**, 076 (2002) [arXiv:hep-th/0205144].

[42] B. Feng, A. Hanany, Y. H. He and A. M. Uranga, "Toric duality as Seiberg duality and brane diamonds," JHEP **0112**, 035 (2001) [arXiv:hep-th/0109063].

[43] B. Feng, S. Franco, A. Hanany and Y. H. He, "Unhiggsing the del Pezzo," JHEP **0308**, 058 (2003) [arXiv:hep-th/0209228].

[44] C. V. Johnson, A. W. Peet and J. Polchinski, "Gauge theory and the excision of repulson singularities," Phys. Rev. D **61**, 086001 (2000) [arXiv:hep-th/9911161].

[45] S. Franco, A. Hanany and Y. H. He, "A trio of dualities: Walls, trees and cascades," Fortsch. Phys. **52**, 540 (2004) [arXiv:hep-th/0312222].

[46] M. Aganagic and C. Vafa, "G_2 manifolds, mirror symmetry and geometric engineering," arXiv:hep-th/0110171.